Interspecies variation of larval locomotion kinematics in the genus *Drosophila* and its relation to habitat temperature

Yuji Matsuo[a], Akinao Nose[a,b] and Hiroshi Kohsaka[a*]

[a] Department of Complexity Science and Engineering, Graduate School of Frontier Science, the University of Tokyo, 5-1-5 Kashiwanoha, Kashiwa, 277-8561 Chiba, Japan

[b] Department of Physics, Graduate School of Science, the University of Tokyo, 7-3-1 Hongo, Bunkyo-ku, 133-0033 Tokyo, Japan

* For correspondence: (kohsaka@edu.k.u-tokyo.ac.jp, +81-4-7136-3922)

Abstract

Speed and trajectory of locomotion are characteristic traits of individual species. During evolution, locomotion kinematics is likely to have been tuned for survival in the habitats of each species. Although kinematics of locomotion is thought to be influenced by habitats, the quantitative relation between the kinematics and environmental factors has not been fully revealed. Here, we performed comparative analyses of larval locomotion in 11 *Drosophila* species. We found that larval locomotion kinematics are divergent among the species. The diversity is not correlated to the body length but is correlated instead to the habitat temperature of the species. Phylogenetic analyses using Bayesian inference suggest that the evolutionary rate of the kinematics is diverse among phylogenetic trees. The results of this study imply that the kinematics of larval locomotion has diverged in the evolutionary history of the genus *Drosophila* and evolved under the effects of the ambient temperature of habitats.

Keywords: animal locomotion, larval crawling, the genus Drosophila, kinematics, evolution

Introduction

Kinematics of animal locomotion is a critical trait enabling each species to survive in their habitats (Alexander, 2006). Movement patterns have been sculpted during their evolution by adaptation to their environments, and could have diverged among species (Kappeler, 2010). Comparative analyses have identified several examples of differences in the kinematics of locomotion within a group of related species, including insects (Theunissen et al., 2015), reptiles (Fuller et al., 2011), birds (Stoessel & Fischer, 2012), and primates (Thompson et al., 2018). To take an example, two gecko species inhabiting either sandy or rocky environments have been shown to exhibit distinct postures (Fuller et al., 2011). Whereas the interspecies divergence in locomotion patterns can be observed in various phylogenetic branches of the animal kingdom, quantitative comparative analyses of

locomotion kinematics remain limited.

Flies of the genus *Drosophila* have long been used as a model to study interspecific diversification and evolution (Markow & O'Grady, 2005). One salient example of the interspecific variations in the genus *Drosophila* is food for larvae. Some species eat multiple kinds of foods ("generalists" including *Drosophila melanogaster*) while others have strong preferences in food ("specialists" including *Drosophila sechellia*, which has specialized to feed on Morinda fruits) (Markow, 2015; Watada et al., 2020; Watanabe et al., 2019). These diverged species in the genus *Drosophila* offer an opportunity to perform interspecific comparisons in various animal traits including larval locomotion.

Fly larvae, or maggots, have been widely used in the study of the kinematics of locomotion (Berrigan & Lighton, 1993; Berrigan & Pepin, 1995; Fox et al., 2006; Green et al., 1983; Ruiz-Dubreuil et al., 1996; Sokolowski, 1985; Sokolowski et al., 1997). Among the fly species, *Drosophila melanogaster* (*Dmel*) is one of the most examined species, especially by virtue of the availability of resources in genetics and connectomics (Ohyama et al., 2015; Schneider-Mizell et al., 2016; Simpson & Looger, 2018; Venken et al., 2011). *Dmel* larvae locomote by a sequence of forward crawling, and changes of crawling direction achieved by bending their bodies (Green et al., 1983). The kinematics of larval locomotion is affected by ambient temperature (Kwon et al., 2010; Liu et al., 2003; Ohyama et al., 2013; Rosenzweig et al., 2005a). In thermotaxis behaviour in temperature gradient environments, larvae regulate the length of crawling runs between turns and the size and direction of turns (Luo et al., 2010), and the probability of turns is also affected by ambient temperature gradients (Klein et al., 2015). In contrast to the intensive studies on larval behavior in *Dmel*, locomotion kinematics in the larvae of its sister species in the genus *Drosophila* remains unclear.

Here we conducted an interspecies comparison of the kinematics of larval locomotion in the genus *Drosophila*. We address two questions in this study: are locomotion kinematics of larvae similar among *Drosophila* species?; and, if the kinematics are diverged,

68 what factors are related to the diversity? To this aim, we recorded locomotion of larvae of 11
69 *Drosophila* species and extracted kinematic parameters using the tracking software
70 FIMTrack (Risse et al., 2017). Clustering analysis with Jensen-Shannon divergence and
71 statistical analyses show that two kinematics parameters (bend probability and crawling
72 speed) differ among the *Drosophila* species. We found that kinematics varies with habitat
73 temperature but not with body size. The relationship between the kinematics and minimum
74 habitat temperature held at two distinct ambient temperatures: 24°C and 32°C. Phylogenetic
75 analyses of these kinematics, based on Bayesian inference (Hohna et al., 2016), suggests
76 that the rate of evolution of the kinematics is diverged among phylogenetic branches. Among
77 eight traits we tested, the evolution of the crawling speed at 24°C and 32°C were correlated.
78 Consequently, our results suggest that the kinematics of larval locomotion in the genus
79 *Drosophila* diverged in response to environmental variation in ambient temperature.
80

81 **Results**

82 **Kinematic analysis of crawling and bending behaviour in *Drosophila* larvae**

83 In this study, we analyzed the kinematics of larval locomotion. To this aim, we
84 recorded the locomotion of fly larvae that were crawling freely on an agarose substrate stage
85 on a temperature-controlled plate (Figure 1A; see Method section for details). We placed
86 eight to ten larvae at the centre of the stage, which was kept at 24°C, illuminated them with
87 infrared light, which is invisible to fly larvae and does not affect their behaviour, and recorded
88 larval locomotion for three minutes at five frames per second (Figure 1B). Maximum
89 projection of the time-series images shows traces of larval locomotion as multiple curves of
90 multiple larvae (Figure 1C). In an example of *Drosophila melanogaster* (Figure 1D), the
91 traces show smooth curved lines interconnected with angles where larvae exhibit turning
92 behaviour and change crawling direction, which is consistent with previous studies (Berni et
93 al., 2012; Gershow et al., 2012; Gomez-Marin et al., 2011; Gomez-Marin & Louis, 2014;
94 Green et al., 1983; Sims et al., 2019; Tastekin et al., 2015). Larvae under these conditions

predominantly exhibit forward locomotion in which muscular contraction is propagating from the posterior to anterior segments. Characteristics of larval locomotion can be described by two measures: the bend angle and centroid speed (Gershow et al., 2012; Gomez-Marin et al., 2011). The bend angle measures the angle of body axis bending (Figure 1E) and the centroid speed is the speed of the position of the larval centroid (Figure 1F). To obtain these values for each larva at each time frame, we used the object tracking software for small animals, FIMTrack (Risse et al., 2017). The turning behaviour can be detected by the change in the angle of the body axis (Figure 1E) and the reduction in the centroid speed (Figure 1F), as reported previously (Gershow et al., 2012; Gomez-Marin et al., 2011). Accordingly, we used the bend angle and centroid speed for quantitative analysis of larval locomotion in this study.

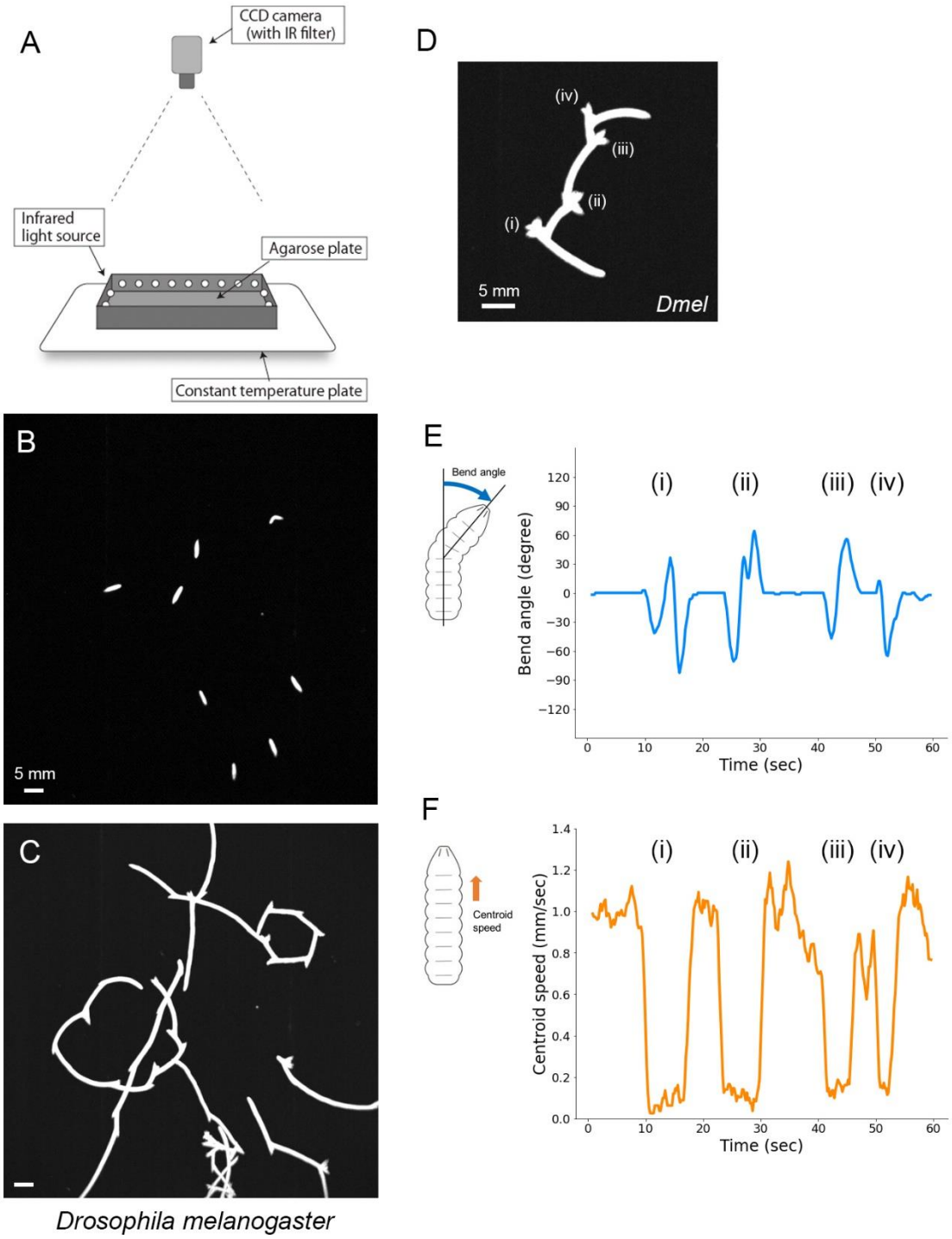

Figure 1. Measurement of larval crawling. (A) Setup of the recording of larval crawling with infrared light and temperature control plate. (B) An example image of multiple larvae recorded

by the setup (A). (C) The trajectories of larval locomotion of *Drosophila melanogaster* recorded for two minutes. (D) A trajectory of single *Drosophila melanogaster* locomotion. Locations where the larva changes its direction are labelled (i) to (iv). (E and F). Bend angle (E) and centroid speed (F) of the larva in (D). Labels (i) to (iv) correspond to those in (D).

Classification of locomotion properties in the genus *Drosophila*

For interspecies comparison of *Drosophila* larval locomotion, we collected 11 fly species in the genus *Drosophila*, whose genome sequences have been read (A. G. Clark et al., 2007; Miller et al., 2018), and for which living individuals are available from fly stock centres (KYORIN-Fly, Fly Stocks of Kyorin University; KYOTO Stock Center (DGRC) at the Kyoto Institute of Technology). The 11 *Drosophila* (*D.*, hereafter) species consist of *D. ananassae* (*Dana*)*, D. erecta* (*Dere*)*, D. mauritiana* (*Dmau*)*, D. melanogaster* (*Dmel*)*, D. mojavensis* (*Dmoj*)*, D. persimilis* (*Dper*)*, D. pseudoobscula* (*Dpse*)*, D. sechellia* (*Dsec*)*, D. virilis* (*Dvir*), *D. willistoni* (*Dwil*) *and D. yakuba* (*Dyak*). Nine species (all but *Dvir* and *Dmoj*) are classified as subgenus *Sophophora* and the remaining two (*Dvir* and *Dmoj*) are *non-Sophophora* species. We plotted the centroid speed and bend angle of freely crawling larvae of each species (Figure 2A). In all the cases, data points accumulated around a region where the bend angle is zero (Figure 2A), which reflects an observation that larvae do not bend during the majority of the time (Figure 1D). We noticed that the deviations from zero in bend angle axis are different among species. For example, data points in *Dvir* are scattered along the bend angle axis more than those in *Dwil* (Figure 2A). To quantify similarities in the distribution of the two-dimensional plots among the species, we calculated Jensen-Shannon divergence, which measures the similarity of two probability distributions (Lin, 1991). We classified the 11 species based on the similarity in the probability distribution of the crawling speed and bend angle plots by hierarchical clustering (Figure 2B and 2C). The classification analysis shows that four species (*Dmel, Dvir, Dmoj and Dper*) form a cluster. These four species show scattered data points along the bend angle axis compared with the other seven

species (Figure 2A). This observation suggests that the kinematics of larvae in the genus *Drosophila* is diverse among species.

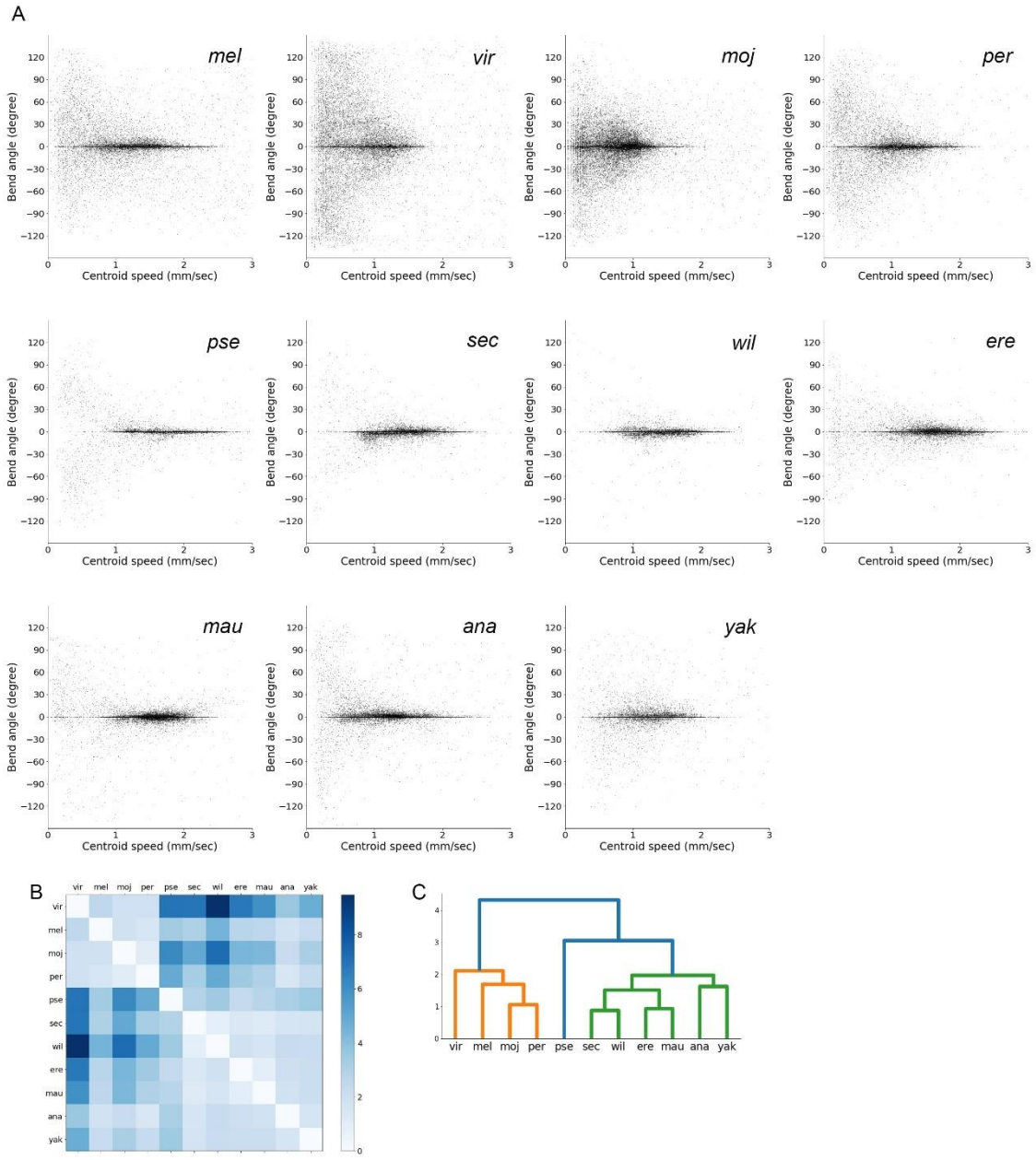

Figure 2. Interspecific comparison of kinematics of larval crawling in the genus *Drosophila*. (A) Plots of the speed of the centroid of larvae and the bend angle in the 11 *Drosophila* species. Each point corresponds to a datum of a single larva of a species in a

144 single time frame. The number of larvae in each species is the following: *Dvir*: n=24; *Dmel*:
145 n=24; *Dmoj*: n=30; *Dper*: n=27; *Dpse*: n=19; *Dsec*: n=21; *Dwil*: n=18; *Dere*: n=22; *Dmau*:
146 n=26; *Dana*: n=22; *Dyak*: n=16. (B) Jensen-Shannon divergences of the probability density
147 of (A). (C) Hierarchical clustering of the kinematics of larval locomotion of the 11 *Drosophila*
148 species.
149
150 **Definition of the bend probability and crawling speed**
151 The clustering analysis suggests that the kinematics is divergent among species.
152 To interpret the diversity in terms of locomotion behaviour, we defined two indices: the bend
153 probability and crawling speed. The bend probability measures how often larvae bend their
154 body laterally. We set the minimum angle of bend as 20 degrees, which was used previously
155 (Risse et al., 2013), and labelled larvae that bent more than this threshold angle to the right
156 or left side as "Bending" (Figure 3A and 3B). This threshold allowed us to extract the
157 difference in the bending rate among the species we examined, and we found that while
158 *Dmel* larvae exhibit larger bend angles than this threshold (Figure 3A), the bend angles in
159 *Dwil* larvae are mostly less than the threshold (Figure 3B). We defined the bend probability
160 of each single larva as a ratio of the number of time frames labelled "Bending" to the total
161 frame number. To define the second index crawling speed, we labelled larvae that bent less
162 than the threshold as "Crawling" (Figure 3A and 3B). We defined the median of centroid
163 speeds of larvae that were labelled "Crawling" as the crawling speed for each single larva.
164 By these definitions, we calculated the bend probability and crawling speed of each larva of
165 the species.
166
167 **Kinematics of larval locomotion is diverse among the *Drosophila* species**
168 We plotted the bend probability of each species (Figure 3C). A statistical analysis
169 shows that the bend probability of the species is diverse ($p = 6.8 \times 10^{-25}$, Kruskal-Walls test).
170 While *Dvir* larvae exhibited frequent bending (bend probability: 0.36 ± 0.05, n = 24), *Dwil*

171 larvae rarely bend (bend probability: 0.003 ± 0.004, n = 18) (Figure 3C). We also plotted the
172 crawling speed of the *Drosophila* species (Figure 3D). The statistical analysis shows that the
173 speed is also diverse among the species ($p = 9.3 \times 10^{-24}$, Kruskal-Walls test). For example,
174 *Dwil* larvae crawl faster than *Dvir* larvae do (crawling speed: 1.46 ± 0.07 mm/sec, n = 24 in
175 *Dwil*; crawling speed: 0.95 ± 0.05 mm/sec, n = 18 in *Dvir*). These analyses indicate that the
176 bend probability and crawling speed are differentiated in the genus *Drosophila*.

177 To capture the trends in the diversity of larval kinematics, we plotted the data in the
178 space of the crawling speed and bend probability (Figure 3E). The graph shows a negative
179 correlation between them (Pearson correlation = -0.76, p = 0.0064). While we used 20
180 degrees as the threshold for defining the bend probability (Figure 3A and 3B), the negative
181 correlation between the crawling speed and bend probability is robust to the choice of the
182 threshold (Pearson correlation = -0.80, p = 0.0030, when the threshold is 10 degrees;
183 Pearson correlation = -0.71, p = 0.014, when the threshold is 30 degrees; Supplementary
184 Figure 1A - 1C). Furthermore, the median of absolute values of bend angle instead of the
185 bend probability exhibits a negative correlation to the crawling speed (Pearson correlation =
186 -0.66, p = 0.026; Supplementary Figure 1D). To sum, the crawling speed and bend probability
187 are diverse among the *Drosophila* species and negatively correlated.

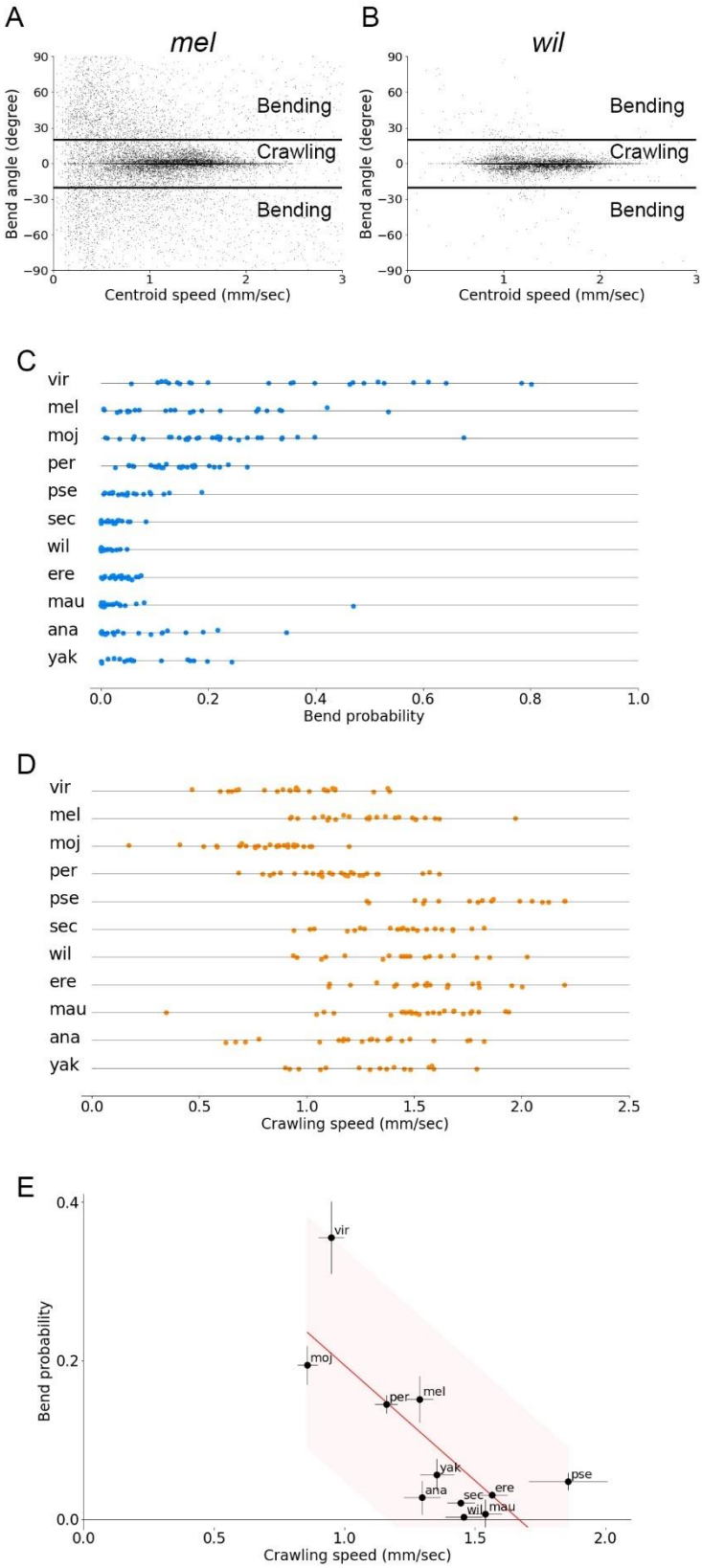
A
mel
B
wil
Bending
Crawling
Bending
Bend angle (degree)
Centroid speed (mm/sec)
C
vir
mel
moj
per
pse
sec
wil
ere
mau
ana
yak
Bend probability
D
Crawling speed (mm/sec)
E
Bend probability
Crawling speed (mm/sec)

189

190 **Figure 3. Bend probability and crawling speed of larval locomotion in the 11**
191 ***Drosophila* species at 24°C and their relationship to habitat temperature of each**
192 **species.** (A and B) Plots of the speed of the centroid of larvae and the bend angle of *D.*
193 *melanogaster* (A) and *D. willistoni* (B). Each point corresponds to a datum of a single larva
194 of a species at a single time frame. Thick horizontal lines denote the threshold between
195 crawling and bending. (C) Bend probability of individual larvae of each species. (D) Crawling
196 speed of individual larvae of each species. Sample numbers in (C) and (D) are the following:
197 *Dvir*: n=24; *Dmel*: n=24; *Dmoj*: n=30; *Dper*: n=27; *Dpse*: n=19; *Dsec*: n=21; *Dwil*: n=18; *Dere*:
198 n=22; *Dmau*: n=26; *Dana*: n=22; *Dyak*: n=16. (E) Scatter plot of bend probability at 24°C
199 against crawling speed at 24°C. Median ± sem is shown. The red line shows the linear
200 regression function and the shaded area represents the 95% confidence band. The point
201 estimate of the Pearson correlation and its 95% confidence interval is -0.76 and [-0.94, -0.30].
202

203 **Comparison between intraspecies and interspecies variability**

204 The comparison of the 11 *Drosophila* species represents the natural variability in
205 larval locomotion across them. Here, it should be noted that we used a single strain for each
206 species in the analysis. For that, the variability appeared above could result not only from
207 interspecies but also intraspecies diversity. Even if there was no interspecies variability,
208 sampling data from population with high intraspecies variation could lead to an apparent
209 diversity across the species. To address this issue, we compared intraspecific deviation with
210 interspecific variability. If intraspecific diversity is a dominant factor for the variability, the
211 deviation within species should be comparable to that among species. In contrast, if
212 interspecific diversity is a major cause, the deviation within species would be smaller than
213 that across species. We examined intraspecies variation in two species in subgenus
214 *Sophophora* (*Dmel* and *Dana*) and one *non-Sophophora* species (*Dvir*) (Figure 4). Two
215 isofemale strains of each species were obtained from the Kyorin stock centre and the larval

216 kinematics of them were measured. To evaluate the contribution of the interspecific
217 deviations to the total deviations, we conducted the analysis of variance (ANOVA). We found
218 a significant interspecific difference in the bend probability (p=0.008, the one-way ANOVA)
219 although the difference in the crawling speed was marginal (p = 0.08, the one-way ANOVA).
220 This observation implies the existence of interspecies diversity in larval locomotion.
221

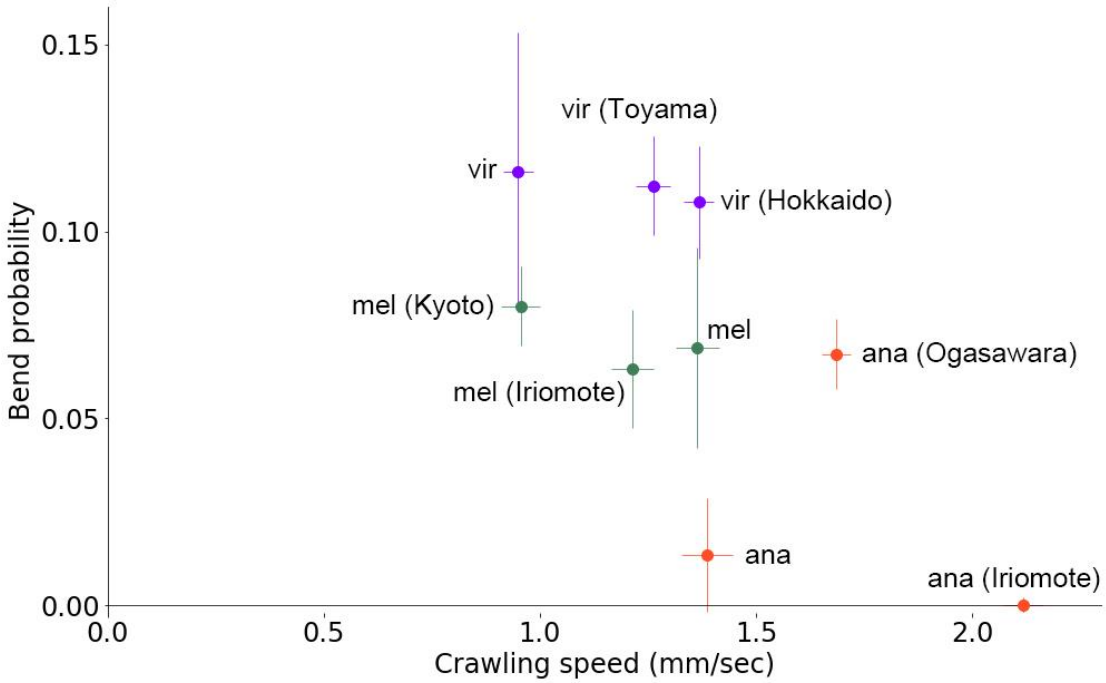

222

223 **Figure 4. Intraspecific comparison in larval locomotion.** Scatter plot of bend probability
224 at 24°C against crawling speed at 24°C of nine strains from three species. Sample numbers
225 are the following: *Dvir*: n=44; *Dvir* (Hokkaido): n=32; *Dvir* (Toyama): n=35; *Dmel*: n=33; *Dmel*
226 *(Kyoto)*: n=47; *Dmel (Iriomote)*: n=33; *Dana*: n=33; *Dana (Ogasawara)*: n=40; *Dana*
227 *(Iriomote)*: n=20.
228

229 **Crawling distance is related to crawling speed and bend probability**

230 In the interspecies variability, there is a negative correlation between the crawling
231 speed and bend probability (Figure 3E). We noticed that this correlation could reflect the

control of the crawling distance by a coordinated change of the crawling speed along with the bend probability. The bend probability is negatively correlated with the crawling distance since frequent bending shortens the distance larvae progress in one direction (Figure 5A) whereas it is obvious that the crawling speed is positively correlated with the crawling distance (Figure 5B). Accordingly, high crawling speed and low bend probability, which are a combination appeared in the negative correlation of them (Figure 3E) both contribute to the increase in the crawling distance. To check whether these geometrical speculations hold in the locomotion of larvae, we examined the relationship between the kinematic parameters and the crawling distance (Figure 5C and 5D). Consistent with the conjecture, the crawling distance is larger when either the bend probability is lower (Figure 5C; Pearson correlation = -0.78) or the crawling speed is higher (Figure 5D; Pearson correlation = 0.67). These observations imply that the coordinated changes in the crawling speed and bend probability would be related to the change in the crawling distance of larvae of each species.

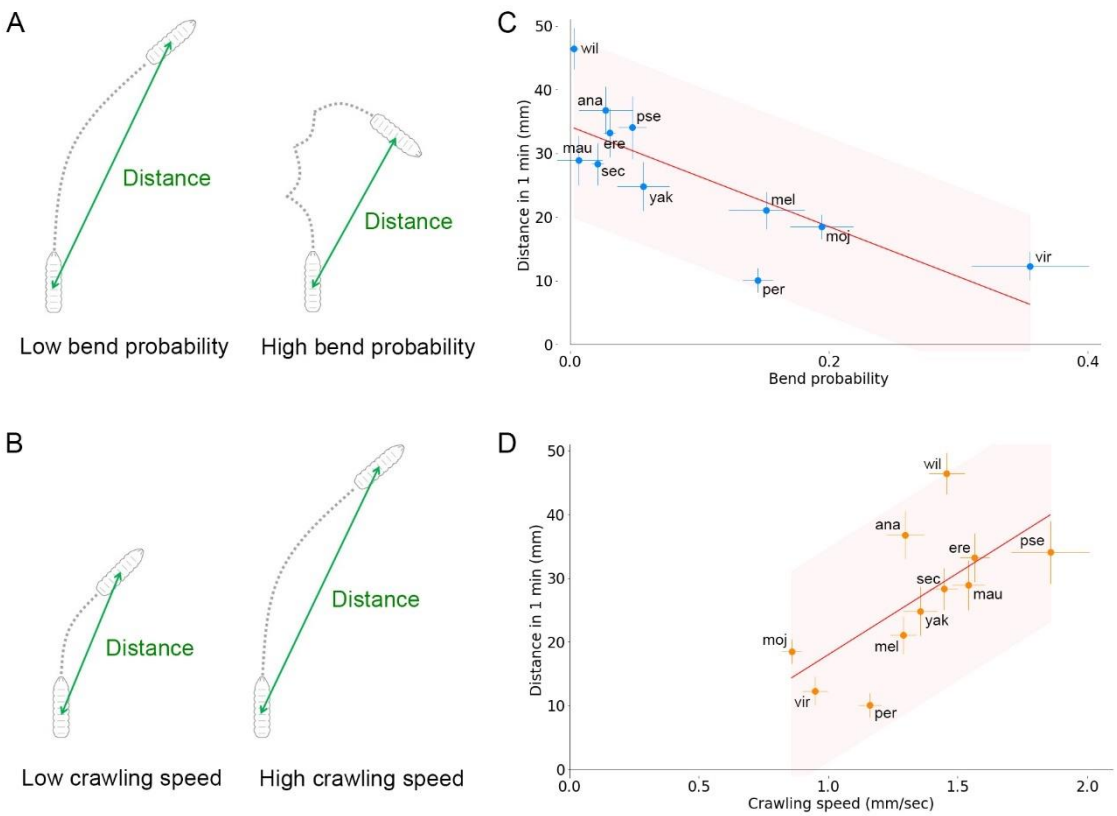

246

247 **Figure 5. Relationship between crawling distance and the two kinematic parameters**
248 **in the 11 Drosophila species.** (A) Schematics of the relationship between the bend
249 probability and crawling distance. (B) Schematics of the relationship between the crawling
250 speed and crawling distance. (C) Scatter plot of the bend probability and crawling distance
251 in one minute in the 11 species. (D) Scatter plot of the crawling speed and crawling distance
252 in one minute in the 11 species. The source locomotion data are the same as in Figure 3C
253 and 3D. In C and D, the red lines show the linear regression functions and the shaded areas
254 represent the 95% confidence bands. The point estimates of the Pearson correlation and
255 their 95% confidence intervals are -0.78 and [-0.94, -0.34] in C and 0.67 and [0.11, 0.91] in
256 D.

257

258 **No relationship between the kinematics of larval locomotion and the body length nor**
259 **phylogenetic relationship**

260 Next, we tried to find factors that relate to the diversification of larval kinematics
261 among species. Among the factors in the morphological differences and the ecological
262 diversity that might be involved in the kinematics diversity (Theunissen et al., 2015) we
263 examined the body length of larvae as a morphological factor and habitat temperature as an
264 ecological factor. A previous study reported an allometric relationship between the body size
265 and the crawling speed in *Diptera* larvae (Berrigan & Pepin, 1995). The authors analyzed
266 larvae in the order *Diptera*, the average size of which spans from 3.7 mm (*Dmel*) to 15.9 mm
267 (*Sarcophaga bullata*). We tested whether the relationship between the body length and the
268 crawling speed also holds within the genus *Drosophila*, a subgroup of the order *Diptera*. The
269 length of the *Drosophila* larvae we used spanned from 3.49 ± 0.05 mm (*Dyak*) to 5.68 ± 0.16
270 mm (*Dpse*) (Supplementary Figure 2A). We found no significant relationship between the
271 body length and crawling speed (Supplementary Figure 2B; Pearson correlation = 0.04, p =
272 0.91) and between the body length and the bend probability (Supplementary Figure 2C;

Pearson correlation = 0.55, p = 0.077). These data suggest that larval length is not a significant factor for larval kinematics variation within the genus *Drosophila*.

Phylogenetic relationship can also be a factor that affects the kinematics. To test this issue, we focused on two species groups: the obscura species group and replete species group. *Dper* and *Dpse* belongs to the obscura species group (See Figure 11A). The kinematics of these two sister species are separated in the distribution of the crawling speed and bend probability (Figure 3E). Similarly, two species of the replete species group, *Dvir* and *Dmor* exhibit distinct kinematics (Figure 3E). These observations suggest that phylogenetic relationship is not a major factor in the divergence of the kinematics.

Relationship between the kinematics of larval locomotion and habitat temperature of the *Drosophila* species

Habitat temperature is one of the critical factors influencing species traits (Schmidt-Nielsen, 1997). To test the possible roles of habitat temperature in the evolution of *Drosophila* larval locomotion, we examined the relationship between habitat temperatures and the locomotion kinematics in the genus *Drosophila*. The habitat regions of the 11 species were obtained from the literature (Brake & Baechli, 2008; Makino & Kawata, 2012; Markow & O'Grady, 2005), and climate temperature data were obtained from a global climate dataset, WORLDCLIM (Hijmans et al., 2005) (Figure 6A, Supplementary Figure 3). We examined the relation between larval kinematics (bend probability or crawling speed) and indices of habitat temperatures (Figure 6B and 6C). We used the mode (the most frequent value) of three indices of habitat temperatures: average, maximum, and minimum temperature. In the minimum habitat temperature data of *Dvir* and *Dpse*, we noticed that the mode temperatures were below 0°C, which cannot be a representative habitat temperature for them (Supplementary Figure 3). Accordingly, for a milder and more representative index, we used the warmest peaks in the minimum habitat temperature histogram ("Tmin" in Supplementary Figure 3). Considering uneven distribution of flies within the region demarcated in

Supplementary Figure 3, the temperature of the warmest peak in the minimum habitat temperature may represent the coldest temperature the majority of the population of each species experiences over many years.

We found that the bend probability and crawling speed are both correlated with average habitat temperature Tave (Figure 6B and 6E. Pearson correlation: bend probability vs Tave = -0.73, crawling speed vs Tave = 0.66). We further analyzed whether the maximum and minimum temperature contribute to the correlation. Maximum habitat temperature, Tmax shows no obvious correlation to the kinematics (Figure 6C and 6F. Pearson correlation: bend probability vs Tmax = 0.37, crawling speed vs Tmax = -0.31). In contrast, minimum habitat temperature, Tmin, exhibit stronger correlation than Tmax (Figure 6D and 6G. Pearson correlation: bend probability vs Tmin = -0.81, crawling speed vs Tmin = 0.74). Even after omitting extreme values (*Dvir* in the bend probability data and *Dpse* in the crawling speed data), the correlation remained high (Pearson correlation: the bend probability vs Tmin (without *Dvir*) = -0.69, the crawling speed vs Tmin (without *Dpse*) = 0.78). Furthermore, even considering multiple comparisons (four factors: larval length, Tave, Tmax and Tmin), the correlations between the kinematic parameters and Tmin were statistically significant ($p = 0.039$ in crawling speed vs Tmin, $p = 0.0010$ in bend probability vs Tmin; Bonferroni correction).

The range (or variability) of habitat temperature could also be a critical factor to determine larval kinematics because species that inhabits in highly variable temperature area would be insensitive to the change in the ambient temperature whereas those breeding in a narrow range of temperature would be sensitive to the small shift in the ambient temperature. To test this point, we examined the relationship between the larval kinematics and the range of habitat temperature, the difference between maximum and minimum temperature in their habitat area (Supplementary Figure 4). The range of habitat temperature is correlated with both the bend probability (Pearson correlation = 0.65, $p = 0.030$) and the crawling speed (Pearson correlation = -0.69, $p = 0.0019$). Consequently, the range of habitat temperature

327 could affect the larval kinematics. In the following analysis, we will focus on the minimum
328 temperature Tmin since it showed the most evident correlation to the larval kinematics.
329 It should be noted that the strains we used have been kept at the housed stocks at
330 23 or 20°C (See Materials and Methods), which might affect the innate behaviour in wild type
331 strains. However, comparison between time period after speciation (at least million years ~
332 10^7 generations (Campbell & Ganetzky, 2012; Russo et al., 1995) and that in laboratories
333 (100 years ~ $10^{3.5}$ generations) indicates that the duration in laboratories occupies as small
334 as 0.03% of the time for the evolution of these *Drosophila* strains. In addition, the rearing
335 temperatures in the stock centres were within the range of habitat temperature of each
336 species (Supplementary Figure 3). These rearing conditions imply that the strains we
337 collected from the stock center should possess innate behaviour that was evolved in their
338 habitat.
339 To sum, larvae of species inhabiting moderate environments (where Tmin is 15 to
340 25°C) showed low bend probability and fast crawling, or long crawling distance, whereas
341 those inhabiting cold environments (where Tmin is 0 to 10°C) exhibited frequent bending and
342 slow crawling, or short crawling distance. Especially, species that has lower Tmin than the
343 ambient temperature in this assay (24°C) showed shorter crawling distance, which implies
344 that excess heat stimuli to these species should reduce their crawling distance.
345 In the analysis above, we estimated the indices of habitat temperature from the
346 temperature data in the entire potential habitat of each species because the original habitat
347 of each strain was unclear. To further check the correlation between the larval kinematics and
348 habitat temperature, we examined the relationship between the kinematics and habitat
349 temperature among the strains of which habitat were recorded (Figure 4 and 6H). We used
350 two *Dmel* strains (collected at Kyoto and Iriomote in Japan), two *Dvir* strains (collected at
351 Hokkaido and Toyama in Japan), and two *Dana* strains (collected at Ogasawara and Iriomote
352 in Japan). The habitat temperature at these location for collecting flies is diverse (Figure 6H
353 right). Intriguingly, the strains originated from the north part of Japan, where the minimum

habitat temperature is low, exhibit slower crawling and high bend probability whereas those from the south part of Japan, where the minimum habitat temperature is high, show the opposite trend (Figure 6H left), which is consistent with the observation based on the temperature of the worldwide statistics (Figure 6D and 6G). Consequently, these observations imply that habitat temperature should be one of the leading factors in sculpting the kinematics of larval locomotion in the genus *Drosophila*.

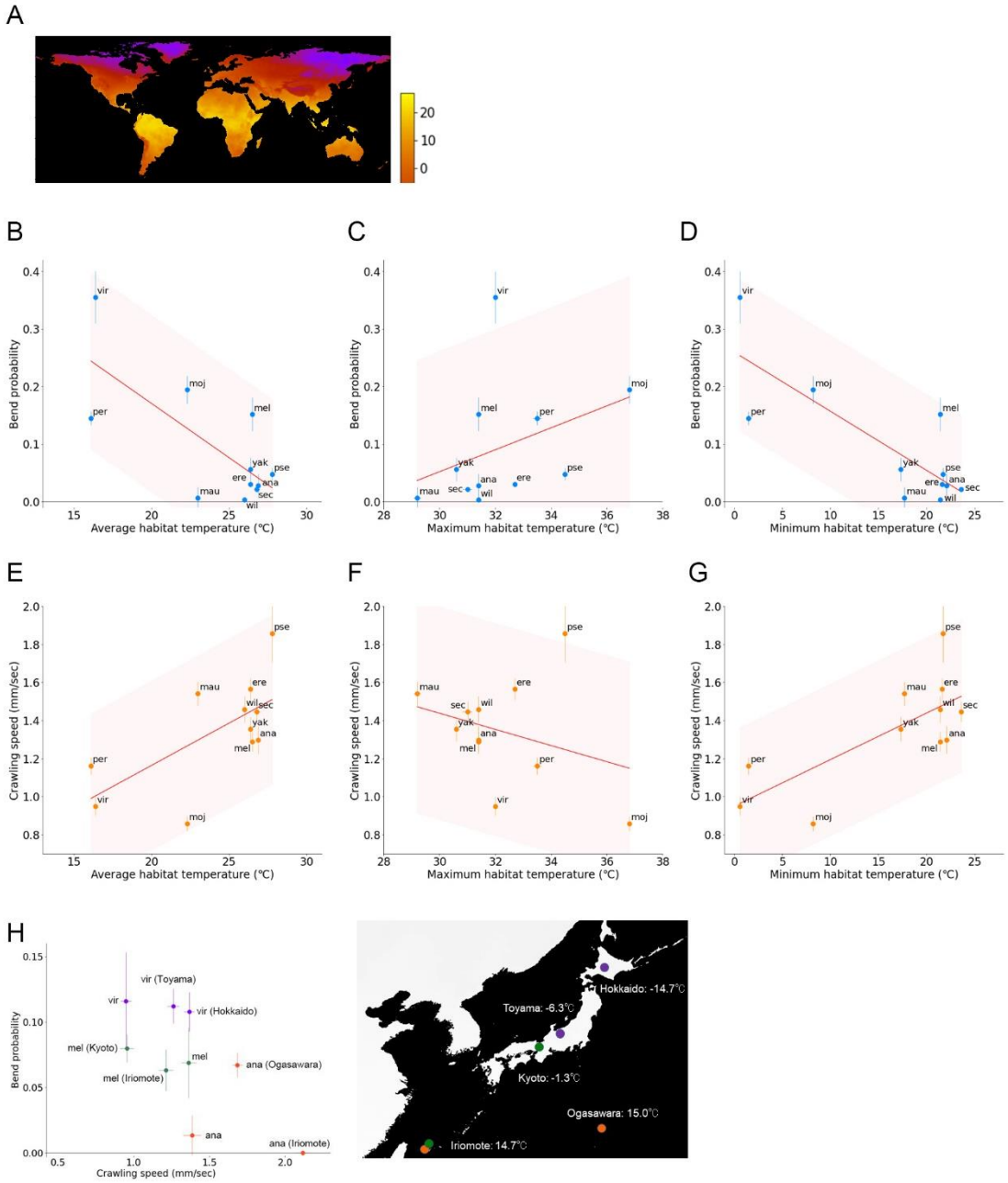

Figure 6. Relationship between the kinematics of larval locomotion and habitat temperature of the Drosophila species. (A) A world map of minimum habitat temperature. (B - D) Scatter plot of the bend probability of the 11 species at 24°C against the average (B), maximum (C), and minimum (D) habitat temperatures. (E - G) Scatter plot of the crawling speed of the 11 species at 24°C against the average (E), maximum (F), and minimum (G)

habitat temperatures. In B to G, median ± sem are shown and the source locomotion data are the same as in Figure 3C and 3D. The red lines show the linear regression functions and the shaded areas represent the 95% confidence bands. The point estimates of the Pearson correlation and their 95% confidence intervals are -0.73 and [-0.93, -0.23] in B, 0.37 and [-0.30, 0.79] in C, and -0.81 and [-0.95, -0.41] in D, 0.66 and [0.09, 0.90] in E, -0.31 and [-0.77, 0.36] in F, and 0.74 and [0.25, 0.93] in G. (H) Left: A scatter plot of intraspecific comparison (the same as Figure 4). Right: A map of Japan representing the minimum habitat temperatures of the six strains shown in the left panel

Correlation between bend probability and habitat temperature among *Drosophila* species at high ambient temperature

So far, we have analyzed larval locomotion at 24°C, which is close to the rearing temperature (See Materials and Methods). Larvae of *Dmel* are known to crawl faster at 32°C than at 25°C (Ohyama et al., 2013). So, we next examined whether the relation between the kinematics indices and habitat temperature holds or not, and how the kinematics indices are changed, at a higher ambient temperature. We performed the same set of measurements and analysis of larval locomotion at 32°C (Figure 7 and 8). The interspecies comparison showed that the bend probabilities at 32°C were correlated with minimum habitat temperature (Figure 7B; Pearson correlation = -0.85, p = 0.0009). To examine the effects of ambient temperature on the bend probability in detail, we compared the differences of bend probability at 24°C and 32°C among the species (Figure 7C). We found no significant relationship between the change in bend probability and the minimum habitat temperature (Figure 7C; Pearson correlation = 0.40, p = 0.22). Seven species showed no significant changes in the bend probability at 32°C (Mann-Whitney U-test of *Dmoj*, *Dper*, *Dpse*, *Dsec*, *Dmau*, *Dana* and *Dyak* in Figure 7A - 7D), while *Dvir* and *Dmel* showed a decrease in the bend probability at 32°C, and *Dwil* and *Dere* exhibited an increase (Mann-Whitney U-test in Figure 7A - 7C, 7E and 7F). Accordingly, we concluded that while the shift of the bend probability between the

394 distinct temperatures is diverse among the *Drosophila* species, the overall trend between the
395 bend probability in relation to habitat temperature holds at the higher ambient temperature of
396 32°C.
397

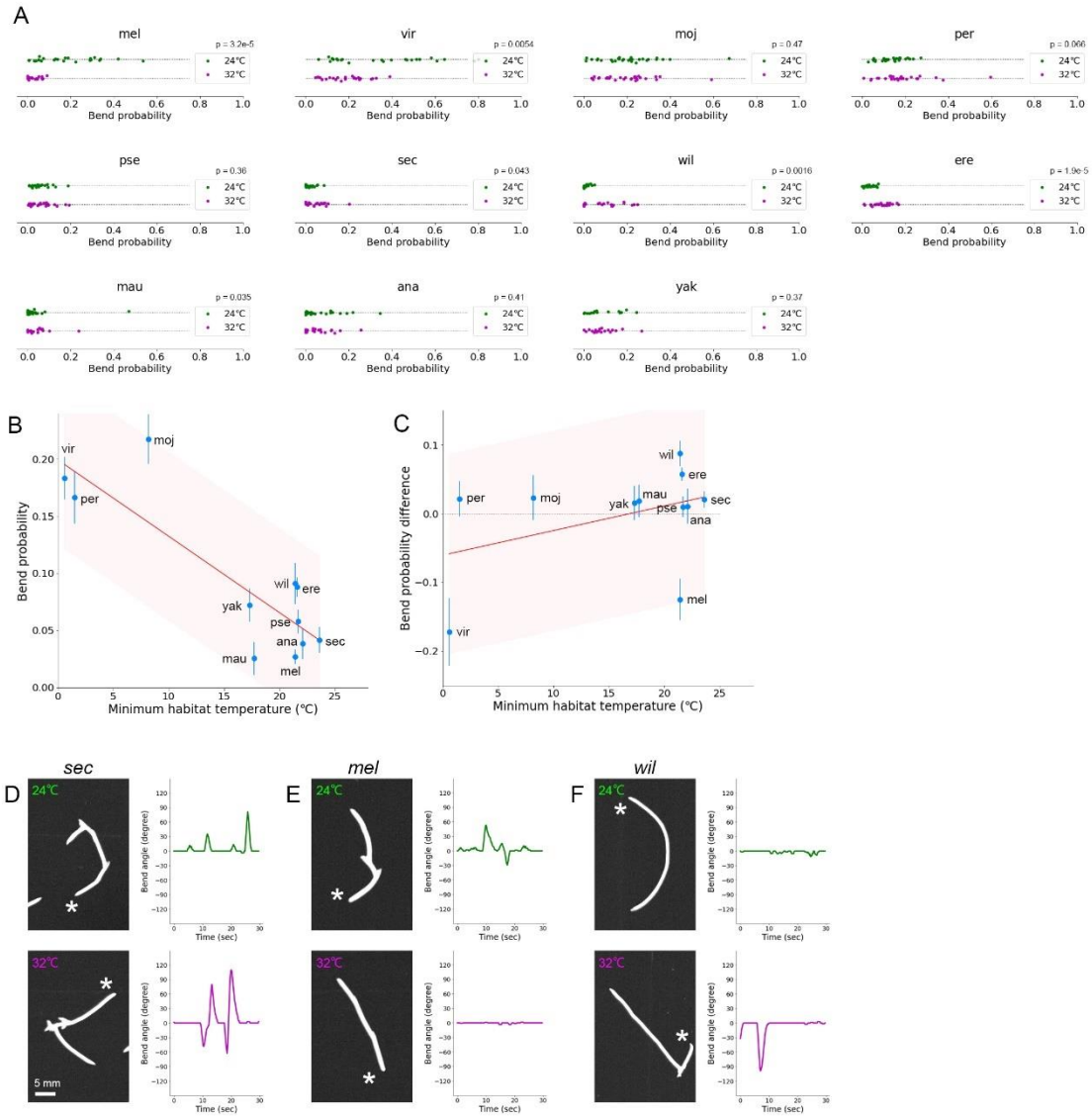

398

399 **Figure 7. Bend probability in larval locomotion in the 11 *Drosophila* species at 32°C.**
400 (A) Bend probability of the 11 species at 24°C and 32°C. The data at 24°C are the same as
401 in Figure 3C. Sample numbers at 32°C are the following: *Dvir*: n=25; *Dmel*: n=20; *Dmoj*:

402 n=29; *Dper*: n=27; *Dpse*: n=25; *Dsec*: n=20; *Dwil*: n=21; *Dere*: n=24; *Dmau*: n=17; *Dana*:
403 n=23; *Dyak*: n=19. P values present the results of Mann-Whitney U-test. (B) Scatter plot of
404 bend probability at 32°C against the minimum habitat temperature, Tmin. (C) Scatter plot of
405 the difference in bend probability between 32°C and at 24°C (bend probability at 32°C – bend
406 probability at 24°C) against the minimum habitat temperature Tmin. In B and C, median ±
407 sem is shown. The red lines show the linear regression functions and the shaded areas
408 represent the 95% confidence bands. The point estimates of the Pearson correlation and
409 their 95% confidence intervals are -0.850 and [-0.96, -0.51] in B and 0.40 and [-0.26, 0.81] in
410 C. (D-F) Examples of trajectories (left) and the bend angle (right) at 24°C (top) and 32°C
411 (bottom) of larval locomotion of each species (D: *Dsec*, E: *Dmel*, and F: *Dwil*).
412

413 **Correlation between crawling speed and habitat temperature among *Drosophila***
414 **species at high temperature**

415 Next, we analyzed the crawling speed at 32°C (Figure 8A). Similar to the bend
416 probability, we found that the crawling speed at 32°C was correlated with the minimum habitat
417 temperature among the species, as it was at 24°C (Figure 8B; Pearson correlation = 0.67, p
418 = 0.024). To examine the effects of ambient temperature on the crawling speed in detail, we
419 compared the difference in the crawling speed at 24°C to 32°C among the species (Figure
420 8C). In contrast to the case in the bend probability, shifts in the crawling speed among the
421 species were common: ten species (all the species but *Dper*) showed a significant increase
422 in crawling speed at 32°C (Mann-Whitney U-test in Figure 8A). *Dper* also exhibited an
423 increase in the crawling speed but it was not statistically significant (Mann-Whitney U-test in
424 Figure 8A). Accordingly, at 32°C, larvae of all the species we tested increased their speed of
425 crawling, which might reflect a general demand to avoid malfunctions in metabolic reactions
426 and dehydration of the body. We also tested the relationship between the change in the
427 speed at 32°C and the minimum habitat temperature for each species (Figure 8C). We found
428 no significant correlation between the speed change and the habitat temperature (Figure 8C;

429 Pearson correlation = 0.07, p = 0.84), which also implies that the speeding-up at high
430 temperature is a general requirement among the species for the larval survival. Accordingly,
431 whereas the details of shifts are different (diverse shift in the bend probability and common
432 shift in the crawling speed among the species), the overall relationship between the kinematic
433 indices and minimum habitat temperature also holds at the higher ambient temperature of
434 32°C.
435

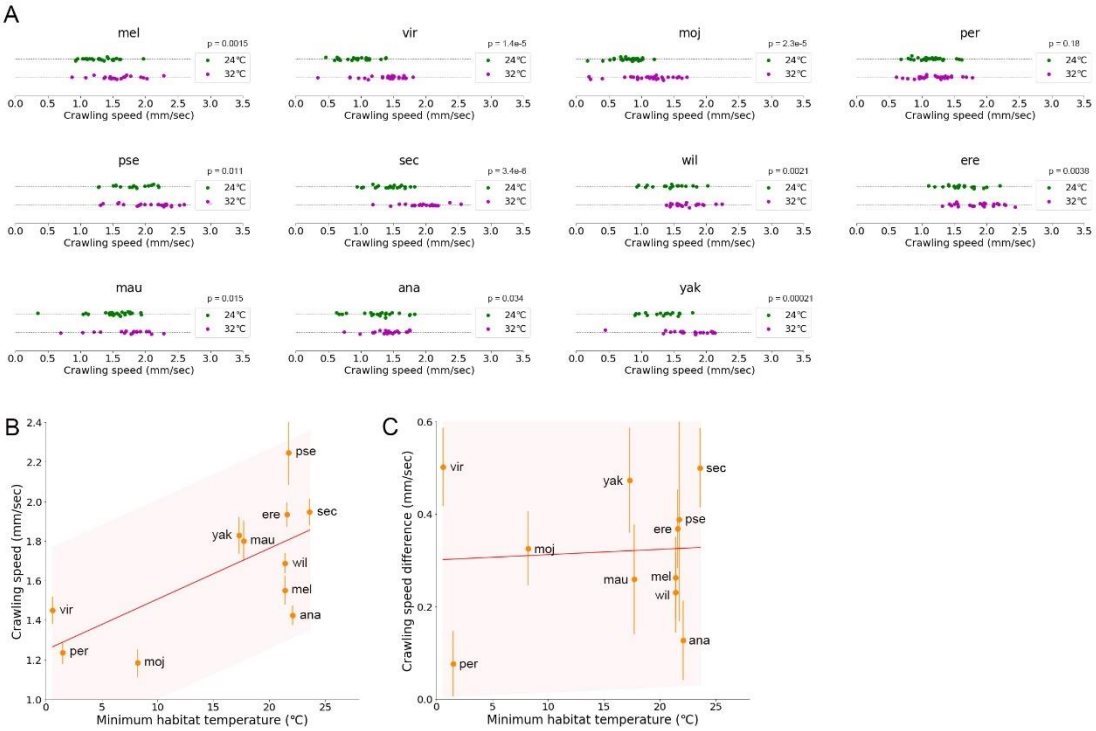

436

437 **Figure 8. Crawling speed of larval locomotion in the 11 *Drosophila* species at 32°C.** (A)
438 Crawling speed of the 11 species at 24°C and 32°C. The data at 24°C are the same as in
439 Figure 3D. Sample numbers at 32°C are the following: *Dvir*: n=25; *Dmel*: n=20; *Dmoj*: n=29;
440 *Dper*: n=27; *Dpse*: n=25; *Dsec*: n=20; *Dwil*: n=21; *Dere*: n=24; *Dmau*: n=17; *Dana*: n=23;
441 *Dyak*: n=19. P values present the results of Mann-Whitney U-test. (B) Scatter plot of the
442 crawling speed at 32°C against the minimum habitat temperature Tmin. (C) Scatter plot of

the difference of the crawling speed between at 32°C and at 24°C (crawling speed at 32°C – crawling speed at 24°C) against the minimum habitat temperature Tmin. In B and C, median ± sem is shown. The red lines show the linear regression functions and the shaded areas represent the 95% confidence bands. The point estimates of the Pearson correlation and their 95% confidence intervals are 0.67 and [0.12, 0.91] in B and 0.07 and [-0.56, 0.64] in C.

A kinematic trend of larval locomotion in the genus Drosophila

To see any gross trend in the shift of larval kinematics in the different species at distinct ambient temperatures, we plotted the kinematics of individual larvae of all the species (Figure 9). At the ambient temperature of 24°C, a trend of kinematics was observed in which the data points were distributed from low crawling speed / high bend probability (the top-left corner in the plot) to high crawling speed / low bend probability (the bottom-right corner in the plot) as the minimum habitat temperature increased (Figure 9A). Intriguingly, the kinematics indices between distinct species were not segregated but rather overlapped. This continuum property can also be observed in the kinematics data at the ambient temperature of 32°C (Figure 9B). According to the modern phylogenetic concept (Markow & O'Grady, 2005), the 11 genus *Drosophila* species in our study consisted of nine subgenus *Sophophora* species (all but *Dvir* and *Dmoj*) and two *non-Sophophora* species (*Dvir* and *Dmoj*). In our plots of kinematics, species in the *non-Sophophora* (*Dvir* and *Dmoj*) were located at the left side in the continuum (Figure 9). This observation implies that the kinematics indices of larvae in *Sophophora* species in the genus *Drosophila* took values in this continuum and kinematics indices in *non-Sophophora* species in the genus *Drosophila* have diverged along this continuum by adaptation to habitat temperature during evolution.

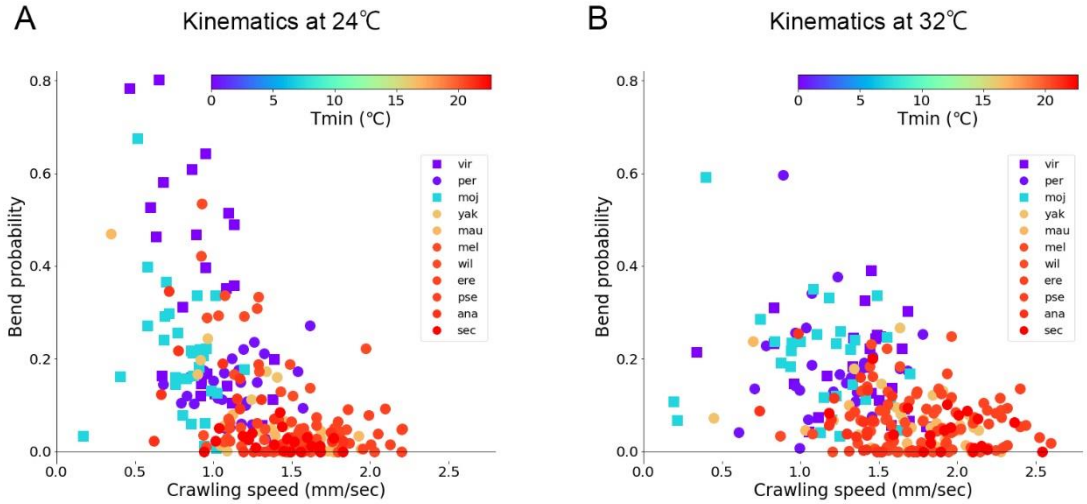

Figure 9. Scatter plot of kinematics in the 11 species at 24°C and 32°C. (A and B) Two dimensional plots of the crawling speed and bend probability. Each point corresponds to data of a single larva of the species. The colour of markers denotes minimum habitat temperature (Tmin) as shown in the color bar. Circles denote *Sophophora* species and squares denote *non-Sophophora* species. The source locomotion data are the same as Figure 3, 7, and 8. A: 24°C, B: 32°C.

No correlation between crawling speed and habitat temperature among *Drosophila* species at an extreme ambient temperature of 40°C

Temperatures of 24°C and 32°C are within the range of natural habitat temperatures of most of the species we tested (Supplementary Figure 3). We next examined larval crawling at an extreme temperature and investigated the relation between the kinematics indices and minimum habitat temperature. Too high a temperature can be noxious for many animals, including *Drosophila* larvae. When *D. melanogaster* larvae are stimulated with a probe heated to 42°C, they exhibit a stereotyped rolling motion as an escape behaviour (Dason et al., 2019; Petersen et al., 2018; Tracey et al., 2003). At below 40°C, on the other hand, larvae

484 do not exhibit rolling behaviour (Petersen et al., 2018), which allows us to study crawling
485 kinematics in this semi-noxious extreme environment. We recorded larval locomotion of the
486 *Drosophila* species at the ambient temperature of 40°C, which corresponds to the highest
487 edge of maximum habitat temperature histograms for many of the species (Supplementary
488 Figure 3). We measured the bend probability and crawling speed of the 11 *Drosophila*
489 species (Supplementary Figure 5 and 6). At the ambient temperature of 40°C, neither the
490 bend probability nor crawling speed was correlated with minimum habitat temperature
491 (Figure 10A and 10B; Pearson correlation: bend probability at 40°C vs Tmin = 0.17, p = 0.61;
492 crawling speed at 40°C vs Tmin = -0.17, p = 0.61). Since 40°C is close to the maximum
493 habitat temperature rather than the minimum habitat temperature, we analyzed the relation
494 between the kinematics indices and maximum habitat temperature instead of minimum
495 habitat temperature. However, neither the bend probability nor crawling speed was correlated
496 with maximum habitat temperature (Pearson correlation: bend probability at 40°C vs
497 maximum habitat temperature = -0.13, p = 0.71; crawling speed vs maximum habitat
498 temperature = -0.10, p = 0.77). Accordingly, the relation between the kinematic indices and
499 habitat temperature does not hold at the extreme ambient temperature of 40°C. This
500 observation suggests that the influence of habitat temperature on the evolution of the
501 locomotion kinematics is restricted within a specific range of ambient temperatures. To
502 examine the effects of the extreme ambient temperature on the kinematics indices in detail,
503 we examined the shift in the bend probability at the distinct temperatures of 40°C and 32°C
504 among the species (Supplementary Figure 5). In seven species, bend probability increased
505 at 40°C. Three species that inhabit moderate temperature areas (*Dvir*, *Dper* and *Dmoj*) and
506 one species that lives on an isolated island (*Dsec*) showed little change in the bend probability,
507 which may reflect a distinct strategy in evolution to cope with the semi-noxious environment.
508 We also examined the shift in the crawling speed at the distinct temperatures of 40°C and
509 32°C among the species (Supplementary Figure 5). We found the crawling speed was
510 reduced at 40°C in all the species (Supplementary Figure 6), which might be a common

adaptation of the *Drosophila* larval locomotion at the extreme ambient temperature and/or due to an abnormal physiological reaction at the semi-noxious temperature. The similar tendency, the increase in the bend probability and the decrease in the crawling speed at 40°C, was also observed when compared with the kinematics at 24°C (Figure 10C and 10D). Intriguingly, in some species, backward crawling, which seldom occurs at 32°C, can be observed at 40°C (Figure 10E). Consequently, these observations show that at the extreme ambient temperature of 40°C, the relation between the kinematics indices and habitat temperature does not hold and larvae exhibit common (increase in the crawling speed) and diverse (changes in the bend probability and generation of backward crawling) shifts in the locomotion kinematics among the *Drosophila* species.

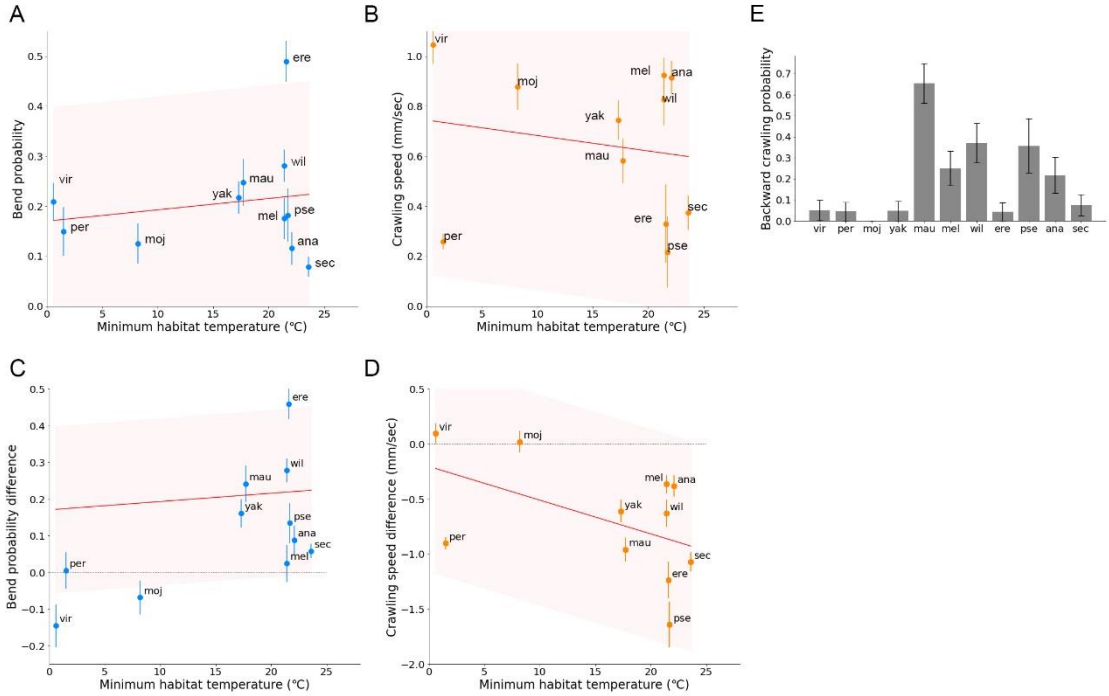

Figure 10. Larval behaviour in the 11 species at 40°C. (A) Scatter plot of the bend probability at 40°C against the minimum habitat temperature Tmin. (B) Scatter plot of the crawling speed at 40°C against the minimum habitat temperature Tmin. (C) Scatter plot of

526 the difference of the bend probability between at 40°C and at 24°C (bend probability at 40°C
527 – bend probability at 24°C) against the minimum habitat temperature Tmin. (D) Scatter plot
528 of the difference of the crawling speed between at 40°C and at 24°C (crawling speed at 40°C
529 – crawling speed at 24°C) against the minimum habitat temperature Tmin. Median ± sem is
530 shown in A - D. Sample numbers for data at 40°C are the following: *Dvir*: n=20; *Dmel*: n=28;
531 *Dmoj*: n=23; *Dper*: n=21; *Dpse*: n=16; *Dsec*: n=27; *Dwil*: n=27; *Dere*: n=22; *Dmau*: n=26;
532 *Dana*: n=23; *Dyak*: n=20. Sample numbers for data at 24°C are the same as Figure 3C and
533 3D. The red lines show the linear regression functions and the shaded areas represent the
534 95% confidence bands. The point estimates of the Pearson correlation and their 95%
535 confidence intervals are 0.17 and [-0.48, 0.70] in A and -0.17, [-0.70, 0.48] in B, 0.17, [-0.48,
536 0.70] in C, and -0.50, [-0.84, 0.15] in D. (E) Backward crawling probability at 40°C of each
537 species. Probability ± standard error based on the binomial distribution are shown. Sample
538 numbers in E are the following: *Dvir*: n=20; *Dmel*: n=28; *Dmoj*: n=23; *Dper*: n=22; *Dpse*:
539 n=14; *Dsec*: n=27; *Dwil*: n=27; *Dere*: n=23; *Dmau*: n=26; *Dana*: n=23; *Dyak*: n=21.
540

541 **Phylogenetic analyses of interspecies differences in kinematics**

542 Finally, to obtain a hint on how the kinematics parameters diversified across the
543 species have developed during the evolutionary history of the genus *Drosophila*, we
544 conducted Bayesian phylogenetic analyses using RevBayes v. 1.0.7 (Hohna et al., 2016;
545 Höhna et al., 2017). At first, we inferred phylogenetic trees of the 11 *Drosophila* species
546 based on eight nuclear genes used previously (Turelli et al., 2018) (See Methods for detail).
547 Then by using our kinematics dataset, we estimated the following three factors in the
548 phylogenetic tree by Bayesian inference: the rate of evolution at each branch of the
549 phylogenetic trees, relative rates of evolution among the kinematic parameters, and the
550 correlation between the kinematic parameter evolutions (Kalay et al., 2020). To perform the
551 inference, we constructed a data matrix of eight parameters (the bend probability at 24, 32
552 and 40°C, the crawling speed at 24, 32 and 40°C, backward crawling probability at 40°C and

553 the body length), for each of the 11 *Drosophila* species. We assumed that these parameters
554 evolve under a multivariate Brownian-motion model (Huelsenbeck & Bruce, 2003; Kalay et
555 al., 2020; Lartillot & Poujol, 2011) (See Methods for detail). We estimated the three factors
556 (the evolution rates at phylogenetic trees, relative evolution rates among the kinematic
557 parameters, and the correlation between the parameter evolutions) by running a Markov
558 Chain Monte Carlo simulation.

559 The phylogenetic analyses indicated that the rates of evolution in the kinematics are
560 highly diverse over branches in the phylogenetic tree (Figure 11A and Supplementary Figure
561 7). In addition, the evolutionary rates are distinct among the eight kinematics parameters
562 (Figure 11B). The bend probability at 24°C and the probability of backward crawling at 40°C
563 have a relatively high evolution rate, which might reflect large diversification of these two
564 parameters among the species (Figure 9A and 10E).

565 Some kinematics traits might have evolved cooperatively. To test this possibility, we
566 calculated the correlation of the evolutionary changes between the kinematic parameters. In
567 the correlation analyses of all pairs of the parameters, the crawling speed at 24°C and the
568 crawling speed at 32°C were the most correlated (Figure 11C). On the other hand, the
569 evolutions of the bend probability between at 24°C and 32°C were less correlated. This
570 observation is consistent with the notion that while changes in the bend probability from 24°C
571 to 32°C among the species are diverse (Figure 7C), all the species show an increase in the
572 crawling speed by the temperature shift (Figure 8C). Consequently, the phylogenetic
573 analyses imply that the kinematics indices of larval locomotion have evolved differently in
574 distinct branches of a phylogenetic tree with keeping a correlation between specific
575 locomotion traits such as crawling speed at distinct temperatures.
576

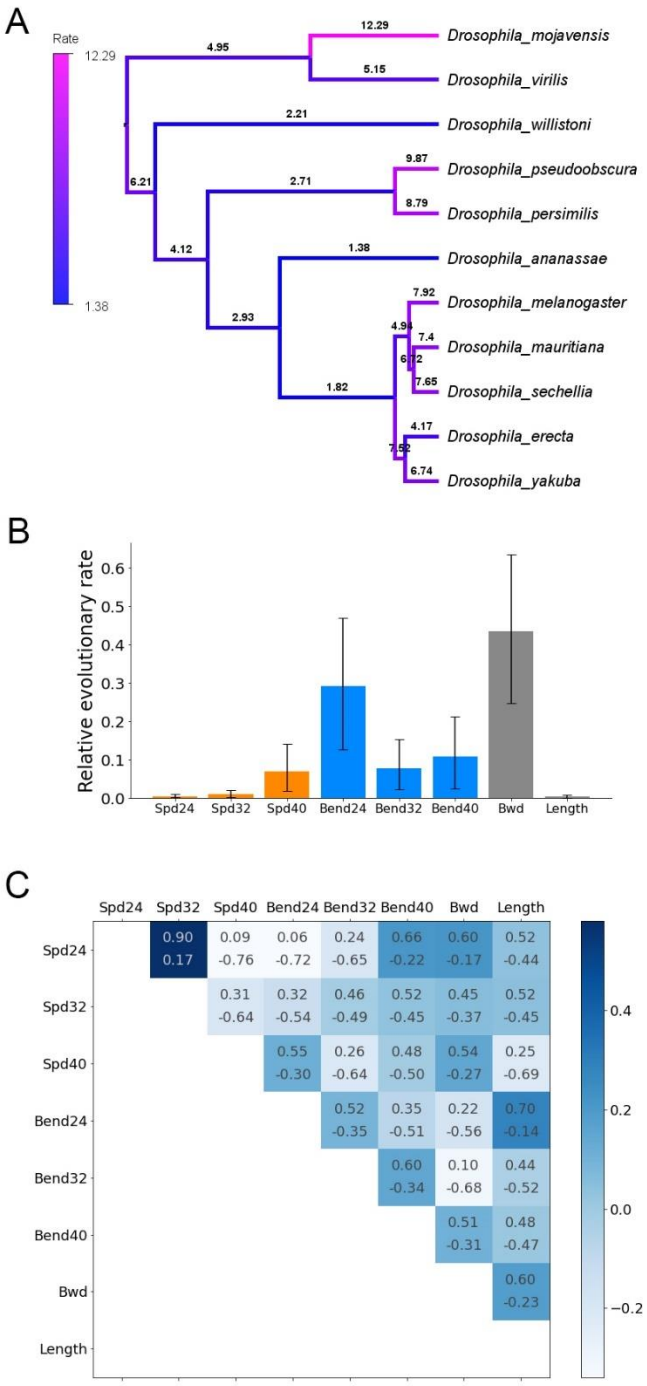

Figure 11. Phylogenetic analyses of larval locomotion in the genus *Drosophila*. (A) Phylogenetic tree estimated from Bayesian inference. The topology is inferred by coding

581 sequences of eight genes of the 11 *Drosophila* species. As a prior distribution for the
582 Bayesian inference, an uncorrelated exponential (UCED) relaxed-clock model was used.
583 Colour and a value of each branch denote the relative rate of the evolution of the eight
584 kinematic traits. (B) Relative evolution rates of the eight kinematics traits estimated by the
585 Bayesian inference. Mean ± 95% highest posterior density is shown. (C) Correlation
586 between the evolution of eight traits. Numbers represent the range of 95% highest posterior
587 density. Abbreviations in (B) and (C) are the following: Spd24: crawling speed at 24°C,
588 Spd32: crawling speed at 32°C, Spd40: crawling speed at 40°C, Bend24: bend probability at
589 24°C, Bend32: bend probability at 32°C, Bend40: bend probability at 40°C, Bwd: probability
590 of backward crawling, Length: axial body length of larvae.
591

592 **Discussion**

593 In this work, we investigated interspecies differences in larval locomotion in the
594 genus *Drosophila*. We used the bend probability and crawling speed as measures to examine
595 larval locomotion. Despite the similar appearance of larval bodies in the different species, the
596 kinematics of larval locomotion is diverged (Figure 2). The body length is not a leading factor
597 for the diversity of kinematics (Supplementary Figure 2). Phylogenetic relationship is also not
598 a major determinant for the kinematics (Figure 3E and 11A). Considering a previous study
599 showing that phylogenetic relationship does not correlate with the divergence in the
600 morphology of larval neuromuscular junctions (Campbell & Ganetzky, 2012), genetic drift with
601 random accumulation of neutral mutations is unlikely to underlie the divergence in the larval
602 crawling patterns. In contrast, habitat temperature correlates with both the bend probability
603 and crawling speed at both 24°C and 32°C ambient temperature (Figure 12), which implies
604 the kinematics indices are adapted to ambient temperature in evolution. Phylogenetic
605 analysis by Bayesian inference suggests that the rates of evolution are divergent among the
606 branches of the phylogenetic tree (Figure 11A). Among the kinematic parameters, the bend
607 probability at the ambient temperature of 24°C and the backward crawling probability at 40°C

608 have relatively higher evolution rates than the others and the evolution of the crawling speed
609 at 24°C and 32°C are correlated (Figure 11B and 11C). Regarding the questions raised in
610 the Introduction section, our results suggest the following: (1) Locomotion kinematics of
611 larvae is divergent among *Drosophila* species. (2) The habitat temperature is more related
612 to the kinematics indices (the bend probability and crawling speed) than the body length
613 (Figure 12).
614

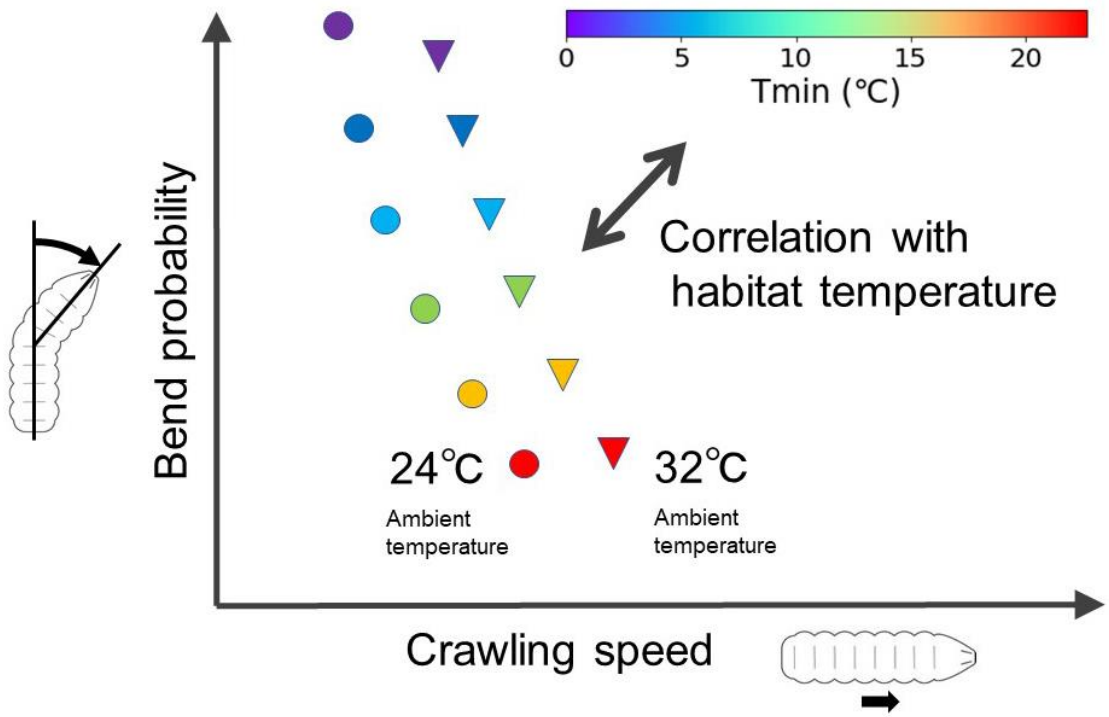

615
616 **Figure 12. Summary of this study.** Disks and triangles denote the kinematics of each
617 species at 24°C and 32°C, respectively.
618
619 To conduct the quantitative analyses, we measured the larval crawling behaviour in
620 simple experimental conditions: at the constant temperatures and humidity levels and on a
621 flat surface of agarose gel. However, the environmental conditions in the wild for *Drosophila*
622 larvae are far more complicated and diverse (Markow, 2015). For example, *Dmoj* breeds in

623 cacti in the desert while *Dvir* inhabits in the slime fluxes in temperate and subarctic climate
624 (Supplementary Figure 3; (Markow, 2015)). Our data in this paper imply that the variation of
625 the kinematics should be related to the diversity of environmental conditions including habitat
626 temperature. Comprehensive and quantitative analyses of larval locomotion in nature would
627 shed light on the causes and meanings of the changes in larval kinematics appeared in the
628 evolution.

629 The correlation between habitat temperature and the kinematics raises a question
630 about the underlying mechanisms of adaptive change in kinematics to the habitat
631 temperature. We presume that the adaptive change was likely to be driven by two factors:
632 the pupation positioning and competition over food. Regarding the pupation behaviour, a
633 previous study showed a correlation between path lengths of crawling and heights of
634 pupation location in *D. melanogaster* (Sokolowski, 1985). Since pupae are immobile,
635 adequate selection of pupation position is vital for their survival. Moisture is one of the key
636 factors that affects the selection of pupation site, since dry environments can cause pupal
637 desiccation, while soaked media might lead to the drowning of pupae (Sokolowski, 1985;
638 Sokolowski et al., 1984). It is reasonable to assume that habitat temperature is a leading
639 factor in determining the moisture levels of microenvironments of *Drosophila* larvae.
640 Accordingly, divergent temperatures in the habitats of flies leads to variability in moisture
641 levels, the ambient moisture affects the pupation position (Sokolowski et al., 1984), and the
642 pupation position is related to the path length of crawling (Sokolowski, 1985). These three
643 links might underlie the relationship between the larval locomotion kinematics and habitat
644 temperature of each species.

645 The second possible mechanism underlying the relation between habitat
646 temperature and locomotion kinematics is related to competition over food. It is suggested
647 that larval feeding is competitive between individuals (Rohlfs & Hoffmeister, 2003). There is
648 a positive relation between fitness and density (called Allee effects) in *D. melanogaster* larvae
649 (Wertheim et al., 2002) and so female flies aggregate eggs when laying them (Rohlfs &

650 Hoffmeister, 2003). Consequently, the larval population tends to be overcrowded (Burnet et
651 al., 1977) and larvae compete over the limited resources to meet their need to consume
652 sufficient amount of nutrient within limited larval periods (Nicholson, 1954). If the available
653 food is limited and larval density is high, larvae need to crawl further (Sokolowski et al., 1997),
654 which can be an evolutionary driving force to increase the crawling distance. In contrast, if
655 there is plenty of food in the habitat, the crawling distance remains unchanged or even
656 decreases during evolution, because crawling behaviour is energetically costly (Berrigan &
657 Lighton, 1993). Consistent with this implication, the diversification in the larval kinematics in
658 the 11 *Drosophila* species gives rise to the variation in the crawling distance (Figure 5).
659 Accordingly, feeding conditions, especially the choice of which foods to eat, can affect
660 kinematics of larval locomotion in evolutionary processes so that the divergence of food to
661 eat can lead to the divergence in locomotion kinematics. In regard to this point, food for larvae
662 of the genus *Drosophila* is divergent and related to their living environments (Markow, 2015;
663 Watada et al., 2020; Watanabe et al., 2019). So, the nutritional conditions (nutrient balances
664 and fermentation etc.) and physical properties (hardness and wetness etc.) of food to eat
665 vary among the *Drosophila* species, which can drive evolutionary divergence in the
666 kinematics of larval locomotion. Then, the growth of plants, including fruits and vegetables,
667 for larvae is strongly affected by habitat temperature. Therefore, divergence in habitat
668 temperature may affect the locomotion kinematics during evolution through divergence in the
669 foods that larvae feed on, and divergence in requisite feeding behaviour for larval growth.
670 Comprehensive kinematics studies of other *Drosophila* species and quantitative analyses of
671 microenvironments of wild larvae in nature will give us insights on the relationships between
672 ambient temperature and diverse larval locomotion kinematics.

673 How can we approach the neural circuit mechanisms underlying the interspecies
674 divergence in larval locomotion? Circuit mechanisms in larval locomotion have been
675 examined intensively in *Drosophila melanogaster*. Recent connectomics studies have
676 identified several key neurons for larval locomotion in *Drosophila melanogaster* (Carreira-

677 Rosario et al., 2018; M. Q. Clark et al., 2018; Fushiki et al., 2016; Heckscher et al., 2015;
678 Hughes & Thomas, 2007; Kohsaka et al., 2014, 2017, 2019; Schneider-Mizell et al., 2016;
679 Tastekin et al., 2015; Zwart et al., 2016). Regarding bending, the thoracic neuromere was
680 shown to be important in bending in chemotaxis (Tastekin et al., 2015). Especially, the
681 commissural connection is crucial for bending (Berni, 2015). In addition, a signal from the
682 chordotonal sensory organ is also required to generate bending (Ainsley et al., 2003).
683 Regarding the crawling speed, a group of inhibitory premotor neurons were identified to be
684 critical (Kohsaka et al., 2014). Proprioceptive feedback and neuromodulation are both
685 important for the normal crawling speed (Fox et al., 2006; Hughes & Thomas, 2007).
686 Furthermore, kinematics of the larval locomotion have been measured and investigated
687 quantitatively in detail (Gepner et al., 2015; Gershow et al., 2012; Gomez-Marin et al., 2011;
688 Gomez-Marin & Louis, 2014; Heckscher et al., 2012; Hernandez-Nunez et al., 2015; Lahiri
689 et al., 2011; Luo et al., 2010) and analysed by mathematical modelling (Gjorgjieva et al.,
690 2013; Loveless et al., 2019; Loveless & Webb, 2018; Pehlevan et al., 2016; Sun et al., 2020).
691 Regarding temperature sensing, neuronal and molecular mechanisms on temperature-
692 guided behaviour have been clarified (Dillon et al., 2009; Klein et al., 2015; Kwon et al., 2008,
693 2010; Liu et al., 2003; Ni et al., 2016; Rosenzweig et al., 2005b, 2008; Shen et al., 2011).
694 These extensive findings on the cellular and molecular mechanisms on larval crawling in
695 *Drosophila melanogaster* will be an ideal starting point to investigate the evolution of larval
696 behaviour in the genus *Drosophila*. For example, differences in commissure fibre tracts in
697 the central nervous system (Berni, 2015) among the species might underlie the divergence
698 in the bend probability. Interspecies comparison of a group of interneurons PMSIs (*period*-
699 positive median segmental interneurons), which are involved in the crawling speed (Kohsaka
700 et al., 2014), would reveal neural mechanisms on the evolutionary diversification in the
701 crawling speed. Comparative analyses of neural network architectures and gene expression
702 among the *Drosophila* species will relate the evolution of the nervous system to the adaptive
703 diversification in larval behaviour.

Materials and Methods

Drosophila strains

We used the following fly stocks (17 strains from 11 species): *Drosophila ananassae* (k-s01), *Drosophila erecta* (k-s02), *Drosophila yakuba* (k-s03), *Drosophila melanogaster* (k-s04), *Drosophila sechellia* (k-s10), *Drosophila persimilis* (k-s11), *Drosophila pseudoobscura* (k-s12), *Drosophila willistoni* (k-s13), *Drosophila virilis* (k-s14) and *Drosophila mojavensis* (k-s15), *Drosophila melanogaster* collected at Kyoto (k-aba029) and Iriomote (k-aba032), *Drosophila ananassae* collected at Ogasawara (k-aaa027) and Iriomote (k-aaa309), and *Drosophila virilis* collected at Hokkaido (E-15601) and Toyama (E-15605) from KYORIN-Fly, Fly Stocks of Kyorin University and *Drosophila mauritiana* (#900020) from KYOTO Stock Center (DGRC) at the Kyoto Institute of Technology. These strains have been maintained at 23°C (except for *Drosophila persimilis* at 20°C) in the stock centres for more than 10 years. All animals were raised on standard cornmeal-based food at 25°C in the authors' laboratory before the experiments for less than three months after the acquisition from the stock centres.

Recording larval locomotion

Third-instar wandering larvae of each strain were picked up and gently washed in deionised water. Residual food on the larvae was brushed off with a paintbrush. An agarose stage (size: 9cm x 9cm x 5mm; 1.5% agarose; RIKAKEN STAR agarose powder #RSV-AGRP-100G) was placed on a temperature-controlled plate (Cool Plate, AS ONE Corporation, Japan) and the temperature of the surface was kept at 24±1°C, 32±1°C or 40±1°C. Eight to ten larvae were placed on the agarose arena with a paintbrush. The larvae were illuminated with infrared light, which larvae cannot see (LDQ-150IR2-850, wavelength = 850 nm, CCS Inc., Japan) and recorded at five frames/sec with a CCD camera (CGE-B013-U, MIGHTEX, Canada; resolution: 1280 pixels x 960 pixels) and an infrared filter (775LP filter, Omega

731 Optical, USA), and saved as a series of bitmap files. In our setting, the scale of image is 0.13
732 mm/pixel. For each of the 17 strains (from 11 species) and at each of the three ambient
733 temperatures, we repeated the measurement three times.
734
735 **Larva tracking**
736 We obtained a time series of bitmap image files by the procedure described above.
737 The bitmap files were converted to tiff format by Fiji (https://imagej.net/fiji). In cases where
738 larvae accumulated at the first frame, we removed the first several images until the larvae
739 dispersed enough to be identified individually. The x and y coordinates of the centroid and
740 the bend angle (Figure 1E) of individual larvae were obtained by using the FIMTrack software
741 (Risse et al., 2017). We used tracking data of single larvae that were continuously tracked
742 for more than 300 frames (which corresponds to one minute). For the intraspecific analysis
743 in Figure 4, single larvae with more than 150 continuous frames were tracked. In case a larva
744 collided with another larva in the middle of the recording and the larva was traced differently
745 before and after the collision with distinct labels, we treated the two traces as two larvae.
746 Crawling speed of each larva was obtained as the median of crawling speed in the whole
747 trace of the larva. Bend probability of each larva was calculated as the ratio of the number of
748 frames showing bending (Figure 3 for the definition of bending) to the total number of the
749 frames of its trace. The data of the three movies for each species/strain were merged. The
750 coordinates and bend angles were smoothed and plotted by Python 3.7. For the visualization
751 of the traces in Figure 1E and 1F, we smoothed the data by a uniform window function with
752 five frames. The number of pixels in single larva ranges from about 150 (*Dyak*) to 500 (*Dpse*)
753 that is sufficient to capture the body bend angles.
754
755 **Clustering analysis of kinematics**
756 For clustering analysis of the plots in Figure 2A, we made a probability distribution.
757 We discretised the centroid speed axis by an interval of 0.1 mm/sec between 0 and 4

mm/sec and the bend angle axis by an interval of two degrees between 0 and 140 degrees, then created 2800 bins in total (40 bins in the speed axis and 70 bins in the bend angle axis). For each scatter plot, we counted the number of points in each bin and obtained probability density by normalisation with the total number of the points. We calculated the Kullback-Leibler divergence (KL) of probability distributions of two species p(bin) and q(bin) as:

$$\mathrm{KL}(\mathrm{p},\mathrm{q}) = \sum_{\mathrm{bin}=1}^{2800} \mathrm{p}(\mathrm{bin}) * \log \frac{\mathrm{p}(\mathrm{bin})}{\mathrm{q}(\mathrm{bin})}.$$

Since KL(p,q) is an asymmetric measure $(\mathrm{KL}(\mathrm{p},\mathrm{q}) \neq \mathrm{KL}(\mathrm{q},\mathrm{p}))$, we calculated the Jensen-Shannon divergence JS, which is a symmetric alternative to the Kullback-Leibler divergence:

$$\mathrm{JS}(\mathrm{p},\mathrm{q}) = \frac{1}{2}\{\mathrm{KL}(\mathrm{p},\mathrm{q}) + \mathrm{KL}(\mathrm{q},\mathrm{p})\} = \mathrm{JS}(\mathrm{q},\mathrm{p}).$$

Based on the Jensen-Shannon divergence, we conducted the hierarchical clustering using Python 3.7 and the SciPy library.

Habitat temperature of the *Drosophila* species

Global climate data were obtained from the WorldClim data website (https://www.worldclim.org/data/worldclim21.html). We used minimum, mean and maximum temperature in the world at a spatial resolution of five minutes (9.25 km x 9.25 km). Habitat regions of each *Drosophila* species were obtained from the literature (Brake & Baechli, 2008; Makino & Kawata, 2012; Markow & O'Grady, 2005) and the DrosWLD-Species database (https://bioinfo.museum.hokudai.ac.jp/db/modules/stdb/index.php?action=tbl&tbl_id=21) and traced them on the world map (2160 pixel x 4320 pixel) obtained from the WorldClim by using Adobe Illustrator software (Adobe Inc., USA). The maps in Supplementary Figure 2 were generated by Adobe Illustrator and the statistics of the temperature within each species' habitat were calculated by Python 3.7.

784 **Statistical analysis**

785 Statistical calculation was conducted by Python 3.7 in the following analyses:
786 Kruskal-Walls test in Figure 3C and 3D, Pearson correlation in Figure 6B, 6C, 7B, 7C, 8B
787 and 8C, Supplementary Figure 2B, 2C, 4B and 5B, and Mann-Whitney U-test in Figure 7A
788 and 8A and Supplementary Figure 5A and 6A.

789

790 **Phylogenetic analyses**

791 We adopted Bayesian statistics for phylogenetic analyses. In all the phylogenetic
792 analyses, we used the software package, RevBayes v.1.0.7 (Hohna et al., 2016).

793 We estimated the *Drosophila* phylogenetic trees (Figure 8A) by using eight nuclear
794 loci from Turelli et al. (2018): *aldolase*, *bicoid*, *enolase*, *esc*, *transaldolase*, *white*, *wingless*,
795 and *yellow*. We used *Scaptodrosophila lebanonensis* (*S. lebanonensis*) as an outgroup.
796 Coding sequences of these genes for all the species except for *D. mauritiana* and *S.*
797 *lebanonensis* were obtained from Kalay et al., (2020). Coding sequences of the genes of *D.*
798 *mauritiana* and *S. lebanonensis* were obtained from the NCBI web site
799 (https://www.ncbi.nlm.nih.gov/). The genes were aligned with MAFFT version 7 (Katoh &
800 Standley, 2013). We selected the eight genes out of twenty genes described in Turelli et al.,
801 (2018) because homologous genes of the other twelve genes were not identified in the
802 genome assembly of *D. mauritiana*. Based on the eight coding sequences of the twelve
803 species, we performed chronogram analyses described in Turelli et al. (2018) and obtained
804 the phylogenetic tree in Figure 8A, where the root is the branch of *S. lebanonensis* and the
805 length of each branch indicates relative time in the evolution. We repeated the phylogeny
806 inference four times to obtain four trees to check the robustness of this inference in the
807 following analysis.

808 Based on the phylogenetic tree obtained above, we analyzed the evolution of
809 kinematics parameters. We used eight parameters (bend probability at 24, 32 and 40°C,
810 crawling speed at 24, 32 and 40°C, backward crawling probability at 40°C, and body length),

for each of the 11 *Drosophila* species. In this analysis, while the topology of the phylogenetic tree is unchanged, the rates of evolution of the kinematic parameters and the rates of evolution of the branches of the phylogenetic tree were estimated by Bayesian inference. We assumed the kinematics parameters evolve under a multivariate Brownian-motion model (Huelsenbeck & Bruce, 2003; Lartillot & Poujol, 2011). This model consists of two components: the relative rates of evolution among the kinematics parameters and the correlation between each pair of the kinematics parameters (Kalay et al., 2020). The Brownian model assumes that the changes in the kinematics parameters during evolution are additive, which has two consequences: 1) parameters can become negative; 2) evolution rates can depend on the scale of the kinematics parameters. To cope with these properties, we adopted log-transformation to the kinematics parameters as described previously (Kalay et al., 2020). This transformation guarantees that the original kinematics parameters (which are exponentials of the log-transformation) remain positive and controls the size issue by transforming additive changes to multiplicative ones (Kalay et al., 2020). For prior models for the evolution rates of the branches, we specified an uncorrelated exponential (UCED) relaxed-clock model, where the rate of each branch is drawn independently from an exponential distribution. We ran the Markov Chain Monte Carlo (MCMC) simulation of UCED with each of the four phylogenetic trees described in the previous paragraph (Figure 11). Consistent results were obtained by another prior model, an uncorrelated gamma (UCG) relaxed clock model (Supplementary Figure 7), which indicates the predictions are robust to the choice of priors.

Acknowledgement

We thank KYORIN-Fly, Fly Stocks of Kyorin University and KYOTO Stock Center (DGRC) at the Kyoto Institute of Technology for providing fly lines, Dr. Takashi Makino for advice about climate data in the world. We thank Ms. Shibahara for tracing habitats of the 11 species. We thank Dr. Masayoshi Watada for critical comments on the paper. This work was supported

by MEXT/JSPS KAKENHI grants (17K19439, 19H04742, 20H05048 to A.N. and 17K07042, 20K06908 to H.K.).

Competing interests

We have no conflicts of interest with respect to the work.

References

Ainsley, J., Pettus, J., Bosenko, D., Gerstein, C., Zinkevich, N., Anderson, M., Adams, C., Welsh, M., & Johnson, W. (2003). Enhanced locomotion caused by loss of the Drosophila DEG/ENaC protein Pickpocket1. *Current Biology*, *13*, 1557–1563. https://doi.org/10.1016/S

Alexander, R. M. (2006). *Principles of Animal Locomotion*. Princeton University Press.

Berni, J. (2015). Genetic dissection of a regionally differentiated network for exploratory behavior in drosophila larvae. *Current Biology*, *25*(10), 1319–1326. https://doi.org/10.1016/j.cub.2015.03.023

Berni, J., Pulver, S. R., Griffith, L. C., & Bate, M. (2012). Autonomous circuitry for substrate exploration in freely moving drosophila larvae. *Current Biology*, *22*(20), 1861–1870. https://doi.org/10.1016/j.cub.2012.07.048

Berrigan, D., & Lighton, J. R. (1993). Bioenergetic and kinematic consequences of limblessness in larval Diptera. *The Journal of Experimental Biology*, *179*, 245–259.

Berrigan, D., & Pepin, D. J. (1995). How maggots move: Allometry and kinematics of crawling in larval Diptera. *Journal of Insect Physiology*, *41*(4), 329–337. https://doi.org/10.1016/0022-1910(94)00113-U

Brake, I., & Baechli, G. (2008). *Drosophilidae (Diptera)*. Apollo Books.

Burnet, B., Sewell, D., & Bos, M. (1977). Genetic analysis of larval feeding behaviour in Drosophila melanogaster: II. Growth relations and competition between selected lines. *Genetical Research*, *30*(2), 149–161. https://doi.org/10.1017/S0016672300017559

Campbell, M., & Ganetzky, B. (2012). Extensive morphological divergence and rapid evolution of the larval neuromuscular junction in Drosophila. *Proceedings of the National Academy of Sciences of the United States of America*, *109*(11). https://doi.org/10.1073/pnas.1201176109

Carreira-Rosario, A., Zarin, A. A., Clark, M. Q., Manning, L., Fetter, R. D., Cardona, A., & Doe, C. Q. (2018). MDN brain descending neurons coordinately activate backward and inhibit forward locomotion. *ELife*, *7*, 1–28. https://doi.org/10.7554/eLife.38554

Clark, A. G., Eisen, M. B., Smith, D. R., Bergman, C. M., Oliver, B., Markow, T. A., Kaufman, T. C., Kellis, M., Gelbart, W., Iyer, V. N., Pollard, D. A., Sackton, T. B., Larracuente, A. M., Singh, N. D., Abad, J. P., Abt, D. N., Adryan, B., Aguade, M., Akashi, H., … MacCallum, I. (2007). Evolution of genes and genomes on the Drosophila phylogeny. *Nature*, *450*(7167), 203–218. https://doi.org/10.1038/nature06341

Clark, M. Q., Zarin, A. A., Carreira-Rosario, A., & Doe, C. Q. (2018). Neural circuits driving larval locomotion in Drosophila. *Neural Development*, *13*(1), 1–10.

https://doi.org/10.1186/s13064-018-0103-z
Dason, J. S., Cheung, A., Anreiter, I., Montemurri, V. A., Allen, A. M., & Sokolowski, M. B. (2019). Drosophila melanogaster foraging regulates a nociceptive-like escape behavior through a developmentally plastic sensory circuit . *Proceedings of the National Academy of Sciences*, 201820840. https://doi.org/10.1073/pnas.1820840116
Dillon, M. E., Wang, G., Garrity, P. A., & Huey, R. B. (2009). Thermal preference in Drosophila. *Journal of Thermal Biology*, *34*(3), 109–119. https://doi.org/10.1016/j.jtherbio.2008.11.007
Fox, L. E., Soll, D. R., & Wu, C. F. (2006). Coordination and modulation of locomotion pattern generators in Drosophila larvae: Effects of altered biogenic amine levels by the tyramine β hydroxlyase mutation. *Journal of Neuroscience*, *26*(5), 1486–1498. https://doi.org/10.1523/JNEUROSCI.4749-05.2006
Fuller, P. O., Higham, T. E., & Clark, A. J. (2011). Posture, speed, and habitat structure: Three-dimensional hindlimb kinematics of two species of padless geckos. *Zoology*, *114*(2), 104–112. https://doi.org/10.1016/j.zool.2010.11.003
Fushiki, A., Zwart, M. F., Kohsaka, H., Fetter, R. D., Cardona, A., & Nose, A. (2016). A circuit mechanism for the propagation of waves of muscle contraction in Drosophila. *ELife*, *5*, 1–23. https://doi.org/10.7554/elife.13253
Gepner, R., Skanata, M. M., Bernat, N. M., Kaplow, M., & Gershow, M. (2015). Computations underlying Drosophila photo- taxis, odor-taxis, and multi-sensory integration. *ELife*, *4*(MAY), 1–21. https://doi.org/10.7554/eLife.06229
Gershow, M., Berck, M., Mathew, D., Luo, L., Kane, E. A., Carlson, J. R., & Samuel, A. D. T. (2012). Controlling airborne cues to study small animal navigation. *Nature Methods*, *9*(3), 290–296. https://doi.org/10.1038/nmeth.1853
Gjorgjieva, J., Berni, J., Evers, J. F., & Eglen, S. J. (2013). Neural circuits for peristaltic wave propagation in crawling Drosophila larvae: analysis and modeling. *Frontiers in Computational Neuroscience*, *7*(April), 1–19. https://doi.org/10.3389/fncom.2013.00024
Gomez-Marin, A., & Louis, M. (2014). Multilevel control of run orientation in Drosophila larval chemotaxis. *Frontiers in Behavioral Neuroscience*, *8*(FEB), 1–14. https://doi.org/10.3389/fnbeh.2014.00038
Gomez-Marin, A., Stephens, G. J., & Louis, M. (2011). Active sampling and decision making in Drosophila chemotaxis. *Nature Communications*, *2*(1). https://doi.org/10.1038/ncomms1455
Green, C. H., Burnet, B., & Connolly, K. J. (1983). Organization and patterns of inter- and intraspecific variation in the behaviour of Drosophila larvae. *Animal Behaviour*, *31*(1), 282–291. https://doi.org/10.1016/S0003-3472(83)80198-5
Heckscher, E. S., Lockery, S. R., & Doe, C. Q. (2012). Characterization of Drosophila larval crawling at the level of organism, segment, and somatic body wall musculature. *Journal of Neuroscience*, *32*(36), 12460–12471. https://doi.org/10.1523/JNEUROSCI.0222-12.2012
Heckscher, E. S., Zarin, A. A., Faumont, S., Clark, M. Q., Manning, L., Fushiki, A., Schneider-Mizell, C. M., Fetter, R. D., Truman, J. W., Zwart, M. F., Landgraf, M., Cardona, A., Lockery, S. R., & Doe, C. Q. (2015). Even-Skipped+ Interneurons Are Core Components of a Sensorimotor Circuit that Maintains Left-Right Symmetric Muscle Contraction Amplitude. *Neuron*, *88*(2), 314–329. https://doi.org/10.1016/j.neuron.2015.09.009
Hernandez-Nunez, L., Belina, J., Klein, M., Si, G., Claus, L., Carlson, J. R., & Samuel, A. D. T. (2015). Reverse-correlation analysis of navigation dynamics in Drosophila larva using optogenetics. *ELife*, *4*(MAY), 1–16. https://doi.org/10.7554/eLife.06225
Hijmans, R. J., Cameron, S. E., Parra, J. L., Jones, P. G., & Jarvis, A. (2005). Very high resolution interpolated climate surfaces for global land areas. *International Journal of Climatology*, *25*(15), 1965–1978. https://doi.org/10.1002/joc.1276
Höhna, S., Landis, M. J., & Heath, T. A. (2017). Phylogenetic inference using RevBayes. *Current Protocols in Bioinformatics*, *2017*(March), 6.16.1-6.16.34. https://doi.org/10.1002/cpbi.22
Hohna, S., Landis, M. J., Heath, T. A., Boussau, B., Lartillot, N., Moore, B. R., Huelsenbeck, J. P., & Ronquist, F. (2016). RevBayes: Bayesian phylogenetic inference using graphical

models and an interactive model-specification language. *Systematic Biology*, *65*(4), 726–736. https://doi.org/10.1093/sysbio/syw021

Huelsenbeck, J., & Bruce, R. (2003). Detecting Correlation between Characters in a Comparative Analysis with Uncertain Phylogeny. *Evolution*, *57*(6), 1237–1247.

Hughes, C. L., & Thomas, J. B. (2007). A sensory feedback circuit coordinates muscle activity in Drosophila. *Molecular and Cellular Neuroscience*, *35*(2), 383–396. https://doi.org/10.1016/j.mcn.2007.04.001

Kalay, G., Atallah, J., Sierra, N. C., Tang, A. M., Crofton, A. E., Murugesan, M. K., Wykoff-Clary, S., & Lott, S. E. (2020). Evolution of larval segment position across 12 Drosophila species*. *Evolution*, *74*(7), 1409–1422. https://doi.org/10.1111/evo.13911

Kappeler, P. (2010). *Animal Behaviour: Evolution and Mechanisms*. Springer.

Katoh, K., & Standley, D. M. (2013). MAFFT multiple sequence alignment software version 7: Improvements in performance and usability. *Molecular Biology and Evolution*, *30*(4), 772–780. https://doi.org/10.1093/molbev/mst010

Klein, M., Afonso, B., Vonner, A. J., Hernandez-Nunez, L., Berck, M., Tabone, C. J., Kane, E. A., Pieribone, V. A., Nitabach, M. N., Cardona, A., Zlatic, M., Sprecher, S. G., Gershow, M., Garrity, P. A., Samuel, A. D. T., & Sternberg, P. W. (2015). Sensory determinants of behavioral dynamics in Drosophila thermotaxis. *Proceedings of the National Academy of Sciences of the United States of America*, *112*(2), E220–E229. https://doi.org/10.1073/pnas.1416212112

Kohsaka, H., Guertin, P. A., & Nose, A. (2017). Neural Circuits Underlying Fly Larval Locomotion. *Current Pharmaceutical Design*, *23*(12), 1722–1733. https://doi.org/10.2174/1381612822666161208120835

Kohsaka, H., Takasu, E., Morimoto, T., & Nose, A. (2014). A group of segmental premotor interneurons regulates the speed of axial locomotion in drosophila larvae. *Current Biology*, *24*(22), 2632–2642. https://doi.org/10.1016/j.cub.2014.09.026

Kohsaka, H., Zwart, M. F., Fushiki, A., Fetter, R. D., Truman, J. W., Cardona, A., & Nose, A. (2019). Regulation of forward and backward locomotion through intersegmental feedback circuits in Drosophila larvae. *Nature Communications*, *10*(1), 2654. https://doi.org/10.1038/s41467-019-10695-y

Kwon, Y., Shen, W. L., Shim, H. S., & Montell, C. (2010). Fine thermotactic discrimination between the optimal and slightly cooler temperatures via a TRPV channel in chordotonal neurons. *Journal of Neuroscience*, *30*(31), 10465–10471. https://doi.org/10.1523/JNEUROSCI.1631-10.2010

Kwon, Y., Shim, H. S., Wang, X., & Montell, C. (2008). Control of thermotactic behavior via coupling of a TRP channel to a phospholipase C signaling cascade. *Nature Neuroscience*, *11*(8), 871–873. https://doi.org/10.1038/nn.2170

Lahiri, S., Shen, K., Klein, M., Tang, A., Kane, E., Gershow, M., Garrity, P., & Samuel, A. D. T. (2011). Two alternating motor programs drive navigation in Drosophila larva. *PLoS ONE*, *6*(8). https://doi.org/10.1371/journal.pone.0023180

Lartillot, N., & Poujol, R. (2011). A phylogenetic model for investigating correlated evolution of substitution rates and continuous phenotypic characters. *Molecular Biology and Evolution*, *28*(1), 729–744. https://doi.org/10.1093/molbev/msq244

Lin, J. (1991). Divergence Measures Based on the Shannon Entropy. *IEEE Transactions on Information Theory*, *37*(1), 145–151. https://doi.org/10.1109/18.61115

Liu, L., Yermolaieva, O., Johnson, W. A., Abboud, F. M., & Welsh, M. J. (2003). Identification and function of thermosensory neurons in Drosophila larvae. *Nature Neuroscience*, *6*(3), 267–273. https://doi.org/10.1038/nn1009

Loveless, J., Lagogiannis, K., & Webb, B. (2019). Modelling the neuromechanics of exploration and taxis in larval Drosophila. *PLoS Computational Biology*, 1–33. https://doi.org/10.5281/zenodo.1432637

Loveless, J., & Webb, B. (2018). A Neuromechanical Model of Larval Chemotaxis. *Integrative and Comparative Biology*, *58*(5), 906–914. https://doi.org/10.1093/icb/icy094

Luo, L., Gershow, M., Rosenzweig, M., Kang, K., Fang-Yen, C., Garrity, P. A., & Samuel, A. D.

T. (2010). Navigational decision making in Drosophila thermotaxis. *Journal of Neuroscience*, *30*(12), 4261–4272. https://doi.org/10.1523/JNEUROSCI.4090-09.2010

Makino, T., & Kawata, M. (2012). Habitat variability correlates with duplicate content of drosophila genomes. *Molecular Biology and Evolution*, *29*(10), 3169–3179. https://doi.org/10.1093/molbev/mss133

Markow. (2015). The secret lives of Drosophila flies. *ELife*, *4*(JUNE), 1–9. https://doi.org/10.7554/eLife.06793

Markow, T. A., & O'Grady, P. M. (2005). *Drosophila: A guide to species identification and use*. Academic Press.

Miller, D. E., Staber, C., Zeitlinger, J., & Hawley, R. S. (2018). Highly contiguous genome assemblies of 15 drosophila species generated using nanopore sequencing. *G3: Genes, Genomes, Genetics*, *8*(10), 3131–3141. https://doi.org/10.1534/g3.118.200160

Ni, L., Klein, M., Svec, K. V., Budelli, G., Chang, E. C., Ferrer, A. J., Benton, R., Samuel, A. D. T., & Garrity, P. A. (2016). The ionotropic receptors IR21a and IR25a mediate cool sensing in Drosophila. *ELife*, *5*(APRIL2016). https://doi.org/10.7554/eLife.13254

Nicholson, A. J. (1954). An outline of the dynamics of animal. *Australian Journal of Zoology*, *2*(1), 9–65.

Ohyama, T., Jovanic, T., Denisov, G., Dang, T. C., Hoffmann, D., Kerr, R. A., & Zlatic, M. (2013). High-Throughput Analysis of Stimulus-Evoked Behaviors in Drosophila Larva Reveals Multiple Modality-Specific Escape Strategies. *PLoS ONE*, *8*(8). https://doi.org/10.1371/journal.pone.0071706

Ohyama, T., Schneider-Mizell, C. M., Fetter, R. D., Aleman, J. V., Franconville, R., Rivera-Alba, M., Mensh, B. D., Branson, K. M., Simpson, J. H., Truman, J. W., Cardona, A., & Zlatic, M. (2015). A multilevel multimodal circuit enhances action selection in Drosophila. *Nature*, *520*(7549), 633–639. https://doi.org/10.1038/nature14297

Pehlevan, C., Paoletti, P., & Mahadevan, L. (2016). Integrative neuromechanics of crawling in D. Melanogaster Larvae. *ELife*, *5*(2016JULY), 1–23. https://doi.org/10.7554/eLife.11031

Petersen, M., Tenedini, F., Hoyer, N., Kutschera, F., & Soba, P. (2018). Assaying Thermo-nociceptive Behavior in Drosophila Larvae. *Bio-Protocol*, *8*(4), 1–12. https://doi.org/10.21769/bioprotoc.2737

Risse, B., Berh, D., Otto, N., Klämbt, C., & Jiang, X. (2017). FIMTrack: An open source tracking and locomotion analysis software for small animals. *PLoS Computational Biology*, *13*(5), 1–15. https://doi.org/10.1371/journal.pcbi.1005530

Risse, B., Thomas, S., Otto, N., Löpmeier, T., Valkov, D., Jiang, X., & Klämbt, C. (2013). FIM, a Novel FTIR-Based Imaging Method for High Throughput Locomotion Analysis. *PLoS ONE*, *8*(1), 1–11. https://doi.org/10.1371/journal.pone.0053963

Rohlfs, M., & Hoffmeister, T. S. (2003). An evolutionary explanation of the aggregation model of species coexistence. *Proceedings of the Royal Society B: Biological Sciences*, *270*(SUPPL. 1), 33–35. https://doi.org/10.1098/rsbl.2003.0002

Rosenzweig, M., Brennan, K. M., Tayler, T. D., Phelps, P. O., Patapoutian, A., & Garrity, P. A. (2005a). The Drosophila ortholog of vertebrate TRPA1 regulates thermotaxis. *Genes and Development*, *19*(4), 419–424. https://doi.org/10.1101/gad.1278205

Rosenzweig, M., Brennan, K. M., Tayler, T. D., Phelps, P. O., Patapoutian, A., & Garrity, P. A. (2005b). The Drosophila ortholog of vertebrate TRPA1 regulates thermotaxis. *Genes and Development*, *19*(4), 419–424. https://doi.org/10.1101/gad.1278205

Rosenzweig, M., Kang, K. J., & Garrity, P. A. (2008). Distinct TRP channels are required for warm and cool avoidance in Drosophila melanogaster. *Proceedings of the National Academy of Sciences of the United States of America*, *105*(38), 14668–14673. https://doi.org/10.1073/pnas.0805041105

Ruiz-Dubreuil, G., Burnet, B., Connolly, K., & Furness, P. (1996). Larval foraging behaviour and competition in Drosophila melanogaster. *Heredity*, *76*(1), 55–64. https://doi.org/10.1038/hdy.1996.7

Russo, C. A. M., Takezaki, N., & Nei, M. (1995). Molecular phylogeny and divergence times of drosophilid species. *Molecular Biology and Evolution*, *12*(3), 391–404.

https://doi.org/10.1093/oxfordjournals.molbev.a040214
Schmidt-Nielsen, K. (1997). *Animal Physiology: Adaptation and Environment*. Cambridge University Press.
Schneider-Mizell, C. M., Gerhard, S., Longair, M., Kazimiers, T., Li, F., Zwart, M. F., Champion, A., Midgley, F. M., Fetter, R. D., Saalfeld, S., & Cardona, A. (2016). Quantitative neuroanatomy for connectomics in Drosophila. *ELife*, *5*(MARCH2016), 1–36. https://doi.org/10.7554/eLife.12059
Shen, W. L., Kwon, Y., Adegbola, A. A., Luo, J., Chess, A., & Montell, C. (2011). Function of rhodopsin in temperature discrimination in Drosophila. *Science*, *331*(6022), 1333–1336. https://doi.org/10.1126/science.1198904
Simpson, J. H., & Looger, L. L. (2018). *Functional Imaging and Optogenetics in Drosophila*. *208*(April), 1291–1309.
Sims, D. W., Humphries, N. E., Hu, N., Medan, V., & Berni, J. (2019). Optimal searching behaviour generated intrinsically by the central pattern generator for locomotion. *ELife*, *8*, 1–31. https://doi.org/10.7554/eLife.50316
Sokolowski, M. B. (1985). Genetics and ecology of Drosophila melanogaster larval foraging and pupation behaviour. *Journal of Insect Physiology*, *31*(11), 857–864. https://doi.org/10.1016/0022-1910(85)90103-9
Sokolowski, M. B., Kent, C., & Wong, J. (1984). Drosophila larval foraging behaviour: Developmental stages. *Animal Behaviour*, *32*(3), 645–651. https://doi.org/10.1016/S0003-3472(84)80139-6
Sokolowski, M. B., Pereira, H. S., & Hughes, K. (1997). Evolution of foraging behavior in drosophila by density-dependent selection. *Proceedings of the National Academy of Sciences of the United States of America*, *94*(14), 7373–7377. https://doi.org/10.1073/pnas.94.14.7373
Stoessel, A., & Fischer, M. S. (2012). Comparative intralimb coordination in avian bipedal locomotion. *Journal of Experimental Biology*, *215*(23), 4055–4069. https://doi.org/10.1242/jeb.070458
Sun, X., Liu, Y., Liu, C., Mayumi, K., Ito, K., Nose, A., & Kohsaka, H. (2020). A neuromechanical model and kinematic analyses for Drosophila larval crawling based on physical measurements. *BioRxiv*.
Tastekin, I., Riedl, J., Schilling-Kurz, V., Gomez-Marin, A., Truman, J. W., & Louis, M. (2015). Role of the subesophageal zone in sensorimotor control of orientation in drosophila larva. *Current Biology*, *25*(11), 1448–1460. https://doi.org/10.1016/j.cub.2015.04.016
Theunissen, L. M., Bekemeier, H. H., & Dürr, V. (2015). Comparative whole-body kinematics of closely related insect species with different body morphology. *Journal of Experimental Biology*, *218*(3), 340–352. https://doi.org/10.1242/jeb.114173
Thompson, N. E., O'Neill, M. C., Holowka, N. B., & Demes, B. (2018). Step width and frontal plane trunk motion in bipedal chimpanzee and human walking. *Journal of Human Evolution*, *125*, 27–37. https://doi.org/10.1016/j.jhevol.2018.09.006
Tracey, W. D., Tracey, W. D., Wilson, R. I., Wilson, R. I., Laurent, G., Laurent, G., Benzer, S., & Benzer, S. (2003). Gene Essential for Nociception. *Cell*, *113*, 261–273.
Turelli, M., Cooper, B. S., Richardson, K. M., Ginsberg, P. S., Peckenpaugh, B., Antelope, C. X., Kim, K. J., May, M. R., Abrieux, A., Wilson, D. A., Bronski, M. J., Moore, B. R., Gao, J. J., Eisen, M. B., Chiu, J. C., Conner, W. R., & Hoffmann, A. A. (2018). Rapid Global Spread of wRi-like Wolbachia across Multiple Drosophila. *Current Biology*, *28*(6), 963-971.e8. https://doi.org/10.1016/j.cub.2018.02.015
Venken, K. J. T., Simpson, J. H., & Bellen, H. J. (2011). Genetic manipulation of genes and cells in the nervous system of the fruit fly. *Neuron*, *72*(2), 202–230. https://doi.org/10.1016/j.neuron.2011.09.021
Watada, M., Hayashi, Y., Watanabe, K., Mizutani, S., Mure, A., Hattori, Y., & Uemura, T. (2020). Divergence of Drosophila species: longevity and reproduction under different nutrient balances . *Genes to Cells*, *June*. https://doi.org/10.1111/gtc.12798
Watanabe, K., Kanaoka, Y., Mizutani, S., Uchiyama, H., Yajima, S., Watada, M., Uemura, T., &

Hattori, Y. (2019). Interspecies Comparative Analyses Reveal Distinct Carbohydrate-Responsive Systems among Drosophila Species. *Cell Reports*, *28*(10), 2594-2607.e7. https://doi.org/10.1016/j.celrep.2019.08.030

Wertheim, B., Marchais, J., Vet, L. E. M., & Dicke, M. (2002). Allee effect in larval resource exploitation in Drosophila: An interaction among density of adults, larvae, and micro-organisms. *Ecological Entomology*, *27*(5), 608–617. https://doi.org/10.1046/j.1365-2311.2002.00449.x

Zwart, M. F., Pulver, S. R., Truman, J. W., Fushiki, A., Fetter, R. D., Cardona, A., & Landgraf, M. (2016). Selective Inhibition Mediates the Sequential Recruitment of Motor Pools. *Neuron*, *91*(3), 615–628. https://doi.org/10.1016/j.neuron.2016.06.031